Histones of Neutrophil Extracellular Traps (NETs) Activate Brain Pericyte via Dectin-1 in Traumatic Brain Injury

Yang-Wuyue Liu
Army Medical University
Jingyu Zhang
Third Military Medical University Daping Hospital and Research Institute of Surgery
Wanda Bi
Army Medical University
Mi Zhou
Army Medical University
Jiabo Li
Chongqing University
Tiantian Xiong
Army Medical University
Nan Yang
Third Military Medical University Daping Hospital and Research Institute of Surgery
Li Zhao
Army Medical University
Xu Tan
Army Medical University
Xing Chen
Third Military Medical University Daping Hospital and Research Institute of Surgery
Yuanguo Zhou
Third Military Medical University Daping Hospital and Research Institute of Surgery
Wenhui He
Army Medical University
Teng Yang
Army Medical University
Hao Wang
Third Military Medical University Daping Hospital and Research Institute of Surgery
Lunshan Xu
Third Military Medical University Daping Hospital and Research Institute of Surgery
Shuang-Shuang Dai (tmmubiodss66@aliyun.com)

Third Military Medical University https://orcid.org/0000-0002-1394-5471

Research

Keywords: Pericyte, Neutrophil, TBI, NETs, Dectin-1

Posted Date: August 31st, 2021

DOI: https://doi.org/10.21203/rs.3.rs-827730/v1

Abstract

Background

Blood-brain barrier (BBB) disruption and leukocyte infiltration are two pathological features post traumatic brain injury (TBI). However, the role of circulating leukocytes in BBB disruption and the crosstalk between them are not fully elucidated. Neutrophil is the most abundant circulating cell type that migrates into brain tissue when TBI occurs instantly, while brain pericyte occupies a strategic position between circulating cell and interstitial space in BBB. Understanding their interactions is essential to provide insight into the intrinsic relationship and identify biological targets for TBI treatments.

Methods

By analyzing brain tissues from TBI patients and mouse TBI model through immunohistochemical method and flow cytometry, we build the relationship between neutrophils, neutrophil extracellular traps (NETs) and brain pericyte. The components of NETs-related medium were investigated by proteomics and metabolomics to decipher the factors directly regulating pericytes. The molecular mechanisms were deeply explored by WB/CHIP/RT-PCR in primary brain pericyte/pericyte cell line MBVP treated with NETs-formed medium or specific NETs components. In mice TBI model, we also explored the possible therapeutic approaches for TBI treatment that targeting at the axis of neutrophil-NETs-pericyte.

Results

NETs formation is highly enhanced post TBI, inducing the appearance of CD11b expressing brain pericyte simultaneously. This novel $CD11b^{+}$ pericyte subset is characterized with increased permeability and pro-inflammatory profiles. Mechanistically, recognition of histones from NETs by Dectin-1 on pericyte contributes to CD11b induction in protein kinase C (PKC)-c-Jun-dependent manner. Transcription factor c-Jun directly binds to the promoter sequence of *CD11b* to enhance its expression in pericyte, conferring pericyte activation, BBB disruption and aggravated neutrophil infiltration post TBI. Either inhibiting NETs formation by Cl-Amidine or blocking Dectin-1 by Laminarin are both beneficial for decreasing neutrophil infiltration and brain pericyte activation post TBI.

Conclusions

These results unfold that “neutrophil-NETs-pericyte” and “histones-Dectin-1-CD11b” are possible cellular and molecular mechanisms for building connection between BBB damage and neutrophil infiltration. Targeting at NETs formation and Dectin-1 are promising treatments for improving neurological outcomes of TBI patients.

Introduction:

Traumatic brain injury (TBI) is a leading cause of death and disability around the world. Until now, there is no specific treatment that targeting at TBI pathological processes even though the mortality and

neurological outcomes of TBI patients have been remarkably improved with utilization of fast and efficient ways toward optimizing physiology [1–3]. In contrast to risk factors and primary injuries that are unchangeable when impact occurs, secondary injuries are fundamental pathological processes that contribute to heterogeneous outcomes and medically tractable when patients are under supervised care at hospital. Two of the secondary injury processes activated by TBI are the unbalanced activation of immune cells and the dysfunction of the blood-brain barrier (BBB), which establish the connection between brain injury and subsequent neurodegenerative disorders in a proportion of TBI patients [4, 5]. The widespread cellular debris and overwhelming cytokine release after brain mechanical damage activate innate immune system instantly after TBI [1]. The activation of cerebral immune cells (microglia, astrocyte) exerts profound effects on neuroinflammation, leaving the circulating peripheral immune cells underestimated. Neutrophil is the most abundant circulating leukocyte that migrates at the injury sites, and involved in the initiation and development of immunological response [6]. It was previously treated as short-lived cell that eliminated debris and pathogens at injury/infection sites, causing indiscriminative damage to the tissue within acute phase. While the time window that neutrophil plays in TBI might be significantly longer than previously thought since several groups reported that neutrophil was detectable in damaged brain 14 days or 1 year after injury/hemorrhage [7–9]. The authors speculated that neutrophils in parenchyma were anti-apoptotic after infiltration and migrated into damaged tissue persistently even though the BBB integrity had been restored. This prompts us to rethink the previous view that BBB remodeling after damage might be the cause rather than consequence that facilitates leukocytes infiltrating into brain tissue [10]. Neutrophil possibly reprogrammes BBB functions while transmigrating in unidentified manner, making it convenient for the following extravasation of peripheral immune cells (T cell, B cell) post TBI.

Back to 1996, a new form of neutrophil death was described when neutrophil was treated with phorbol 12-myritate 13-acetate (PMA), characterized as decondensed chromatin, perforated membrane and spilled nucleoplasm [11]. This phenomenon was ignored until Brinkmann V *et al* presented a novel defense way of neutrophil in 2004, named neutrophil extracellular traps (NETs), representing that this structure was disintegrated deoxyribonucleic acid (DNA) coated with histones and granules [12]. NETs are fundamental weapons for neutrophil catching and killing pathogens, as well as contributors to unintended damages [13, 14]. In the past two decades, accumulating studies have confirmed the existence of NETs under different pathological conditions, including trauma, infection, cancer and so forth [15–18]. It is recently reported that NETs contributes to the development of several diseases from central nervous system (CNS) [8, 19, 20]. Bérézowski V *et al* showed that neutrophils were present in all brain tissues and 50% of them were NETs positive after autopsy of 14 spontaneous intracerebral hemorrhage (SAH) patients. Both neutrophils and NETs were detected within the haematoma but also in the surrounding tissue [7]. NETs formation markers, including citrullinated histone H3 (CitH3), neutrophil-derived DNA segments as well as peptidylarginine deiminase 4 (PAD4) were significantly increased after TBI or SAH, and correlated with the severity [20, 21]. Vaibhav K *et al* presented that NETs were key factors to exacerbate TBI severity through aggravating neurovascular injury. Degrading NETs formation by PAD4 inhibitor or deoxyribonuclease-1 significantly improved BBB integrity and neurological outcome [21].

Furthermore, Yipp BG *et al* proved that NETs generally formed during crawling and transmigrating, casted large interacted areas with vascular units/BBB [22]. However, the functional components and molecular mechanisms of NETs that influence BBB and neurological recovery are still poorly understood due to complicated constituents of NETs. Therefore, finding out potential target cell and molecular mechanism of NETs is important to illustrate the effects on BBB mediated by neutrophil.

The BBB is compact and dense capillary wall that allows few substances going through to the brain, which is made up by endothelial cells, pericytes and astrocytes [5]. Pericytes are surrounded by endothelial basement membrane and astrocytic pseudopodia, forming intensively tight junctions and fine-tuning normal functions of neurovascular unit [23]. Compared to endothelial cells, pericytes are more sensitive and versatile toward inflammatory stimulus, regulating cerebral blood flow dynamics and leukocyte recruitment [24, 25]. Coordinated crosstalk between dysregulated pericytes and other inherent cell types (microglia, astrocyte) also pave the foundation for further pathogenesis, such as glial over-activation and neuronal hyperexcitability [25, 26]. Interestingly, Proebstl D *et al* found that pericyte was the accomplice toward neutrophil under inflammatory conditions, losing its guard function and supporting neutrophil subendothelial crawling [27, 28]. Based on these, it is tempting to speculate that pericyte could be the potential target cells of NETs, which is involved in neutrophil-mediated BBB dysfunction and neutrophil-related neuroinflammation.

To address this issue, we analyzed brain tissues from TBI patients and mouse TBI model to build the relationship between neutrophils, NETs and brain pericyte. Then, the components of NETs-related medium were deeply investigated by proteomics and metabolomics to decipher the factors directly regulating pericytes. The molecular mechanisms were deeply explored by WB/CHIP/RT-PCR in primary brain pericyte/pericyte cell line MBVP treated with NETs-formed medium or specific NETs components. In mice TBI model, we explored the possible therapeutic approaches for TBI treatment that targeting at the axis of neutrophil-NETs-pericyte.

Materials And Methods:

TBI patients: All studies were approved by the Institutional Research Ethics Committee of Army Medical University, and written informed consent was obtained from each patient's relatives in Department of Neurosurgery, Daping Hospital (Army Special Medical Center). Brain specimens were collected from acute middle/severe TBI patients (GCS of 3–9, within 24 hours) while decompressive craniectomy and damaged brain tissue resection were necessary for patients to survive regardless for age, race, gender, or socioeconomic status (listed in Table S1). All samples were de-identified and coded by the attending surgeon before transport to the laboratory. The specimens were processed and stored according to the Principles of Human Samples Preservations from PRC.

TBI mice model: All animal procedures were approved by The Institutional Animal Care and Use Committee at Army Medical University. Adult mixed-sex C57/BL6 mice (age from 6–8 weeks) were provided by Animal Center of Army Medical University and subjected to sham or controlled cortical

impact as we did previously [29]. Briefly, mice were anesthetized using pentobarbital sodium (30mg/kg) and craniotomy was made in the left parietal bone midway (anterior-posterior 2 mm, medial-lateral 2 mm from bregma). The exposed cortex was impacted by automatic BSI impact machine (LinTech, Monrovia, CA, USA) with down stroke (velocity: 2.5 m/s, deformation depth: 3 mm, duration: 150 ms) to construct moderate/severe TBI mice model, which was roughly equal to the severity of TBI patients. Sham-operated mice underwent the same anesthetic and surgical procedures without impact. The skin incision was closed by sterile sutures and mice were put back to clean, warm cage to recover. For drug treatment studies, Laminarin (TLRL-LAM, InvivoGen) and Cl-amidine (S8141, Selleck Chem) dissolved by saline was administered via intraperitoneal injection.

Neutrophil isolation and treatment: Murine neutrophils were isolated from bone marrow as we did before [30]. The purity of harvested cells was more than 98% which was confirmed by FACS with combined markers ($CD11b^+Ly6G^+$). Human neutrophils were sorted by Beckman Coulter with specific markers ($CD11b^+CD14^-CD15^+$) to identify. These cells were washed with PBS for three times and resuspended in Dulbecco's modified Eagle medium (DMEM), containing high glucose and antibiotics without FBS. PMA (100ng/ml, P1585, Sigma-Aldrich) was added to culture medium for 30 min to induce NETs formation. Then the treated cells were washed with DMEM for 3 times and cultured with new DMEM medium (antibiotic and FBS free) for 6 hours. The NETs-formed medium was purified with high speed centrifuge (14000rpm, 4°C) for 20 min to remove neutrophil, and freshly prepared for the following experiments. The medium ratio of NETs-formed medium/ new DMEM was 1:3 according to preliminary test (Figure S4). Under this condition, the medium could induce obvious CD11b expression without strong cytotoxic effects.

Mice brain pericyte isolation and culture: Mouse brain capillary pericyte was freshly isolated and cultured as previously with some modifications [31]. Briefly, the capillaries were seeded by gradual Percoll (P4937, Sigma-Aldrich) centrifugation and cultured with DMEM medium (antibiotic and 10% FBS contained) for 3–4 days until the flask was 70% confluent. Then primary pericyte was harvested by twice digestions: first digestion was to remove contaminated endothelial cells since the endothelial cells were more easily detached from the flask, second digestion was to collect pericyte for the following steps. The collected pericytes were cultured with DEME medium supplemented with pericyte growth factors (1252, ScienCell Research Labaratories) for 3–5 days until the cells were ready for the next experiments.

Culture of murine brain pericyte cell line: The cell line of mouse brain vascular pericytes (MBVP) was purchased from ScienCell Research Labaratories (M1200, San Diego). MBVP cells were cultured with DMEME at subconfluent density according to the supplier's protocol. Histone peptides of Histone 1 (H1917), Histone 3 (12–357) and Histone 4 (12–347) were all purchased from Sigma-Aldrich and dissolved in ddH_2O for the following treatments.

Brain tissue preparation and analytic fluorescence activated cell sorting (FACS): Mice were sacrificed with CO_2 prior to brain dissection. FACS sorting of brain endothelial cells and brain pericytes was performed according to previous study [32]. In Brief, brain tissue was dissected from mice perfused with saline

transcardially and digested with Liberase™ TL Research Grade (05401020001, Sigma Aldrich) and 2 μg/ml DNase I (104159, Roche) for 30 min at 37°C. Cell suspensions subsequently homogenized with grinder and filtered with sieve (200 mesh) to remove undigested tissue blocks. Myelin and debris were removed by 22% Percoll (P4937, Sigma-Aldrich) centrifugation for 10 min, 560×g at 4°C. Pellets with single vascular cells were carefully collected and resuspended with PBS containing 2% FBS. Single cell suspensions from blood, spleen and brain tissue were stained for 30 min at 4°C with specific antibodies (Table S2). The diagrammatic procedure of cell sorting was shown in Figure S5. Flow cytometry data were analyzed with FlowJo software version 11.

MPO-DNA binding experiment: After harvesting brain tissues and peripheral blood from TBI patients, the lysate of brain tissue or neutrophil were incubated with peroxidase-labeled DNA primary antibody (1:25, MAB3868, Millipore) for 2 hours at 4°C. Then the incubated lysate was transferred into MPO (1:500, MA1-80878, Invitrogen) pre-coated ELISA 96-well plates for 1 hour. Finally the absorbance at 405nm were measured for quantify the MPO-DNA binding capacity to evaluate the level of NETs formation as detailed [21].

Transmission electron microscopy (TEM): Preparation of brain ultrathin sections were described previously [30]. Briefly, left brain tissues of sham and TBI mice were cut into small pieces (2mm×2mm), fixed in 0.2% glutaraldehyde and dehydrated through gradient ethanol incubations. Post-fixation was followed with 2% osmium tetroxide and propylene oxide. Then the samples were embedded and allowed to polymerize at 60°C overnight. Ultrathin sections (65-nm-thick) were cut on Leica UC6 ultramicrotome and placed on 200-mesh nickel grids. Finally, sections were washed with distilled water and stained with 2% uranyl acetate and lead citrate. Dried grids were observed and imaged using TECNAI-10 electron microscope.

H&E staining: Mice were anesthetized 24 hours after TBI and transcardially perfused by pre-warmed saline and 4% paraformaldehyde (PFA). Then brain tissues were immediately removed and fixed in 4% PFA for 24 hours at 4°C. Paraffin-embedded sections (10 μm thick) were stained with hematoxylin and eosin (HE) and observed under a microscope (Olympus IX-81; Olympus, Tokyo, Japan).

LC-MS analysis of cell metabolites: A liquid-liquid extraction and liquid chromatography-electrospray ionization tandem mass spectrometry (LC-MS) method was utilized to determining metabolites from cell culture media. Primary isolated murine neutrophils were treated with or without PMA (100ng/ml) for 30 min, then incubated with DMEM (antibiotic and FBS free) for 6 hours. Subsequently, cultured medium were collected by high speed centrifuge and lyophilized for following steps [33]. Each group contains 7 individual samples and differential molecules with p value < 0.05 were screened out.

TMT proteomics analysis of cell cultured medium: Tandem Mass Tags (TMT) labeled quantitative proteomics method was performed to analyze total protein in neutrophil-cultured medium. Proteins with changes greater than 1.5-fold and $P < 0.05$ were considered differentially expressed, and bioinformatics analysis was performed subsequently as previously [34].

Immunohistochemitry: For tissue sections, mice were perfused with 0.9% NaCl transcardially after anesthetization. Then the brain tissues were immediately frozen and embedded with OCT (4583, Tissue-Tek). Brain sections (10μm) were incubated with primary antibodies (Table S2) diluted by 5% BSA (V900933, Sigma-Aldrich) containing 0.1% Triton X-100 (T8787, Sigma-Aldrich). For cell slices, cells were cultured on poly-L-lysine (P6282, Sigma-Aldrich) coated glass slides and treated with specific conditions. Subsequently, cell slices were washed with PBS for 3 times and fixed with cold 4% PFA for 30 min, following incubation of primary antibodies (Table S2) as tissue sections. Finally, samples were stained with DAPI and intended secondary antibodies and photographed by fluorescence microscope (Olympus IX-81).

Quantitative Realtime-PCR: Total RNA extraction of intended cells was achieved by TRIzol Reagent protocol (15596018, Thermo Fisher). RNA samples were reverse transcribed to cDNA using a Reverse Kit (DRR047S, Takara). Quantitative reverse transcription polymerase chain reaction (qRT-PCR) was performed on a Bio-Rad iCycler (Version 3.0A). The sequences of primers were listed in Table S3. Data were presented as fold change versus control group.

Western blotting: Whole-cell lysates were collected and prepared as we did before [30], and western blot procedure was carried out by standard methods. The information of antibodies for specific proteins were listed in Table S2.

TEER measurement: Transwell inserts (polyester membranes, 3μm pore size, ø=6.5mm; Corning, NY, USA) were coated with pericyte cell line MBVP in 24-well plate ($10^5/cm^2$). The Millicell-ERS (Electrical Resistance System, MERS00002, Millipore) was inserted between upper chamber and lower well while measurement took place. TEER values were obtained from continuous impedance measurements as described previously [35]. Once the TEER value of each insert reached above $200\Omega/cm^2$ (typically after 2–3 days), cells were treated with NETs-induced medium as described above or combined with other treatments (as in figure legends), and TEER measurements were obtained every two hours. TEER data were obtained as Ω/cm^2 and presented as percentage (%) by comparing to the value of control group at the beginning.

Evans Blue assay: 2% Evans Blue solution (4 mL/kg, E8010, Solarbio) was IV injected after TBI. The stain was allowed to circulate for 30 minutes, 6 or 24 hours. Afterwards, the mice were sacrificed and transcardially perfused with 50ml of ice-cold PBS. The left injured brain hemisphere was removed and weighed. Then brain tissues were homogenized in 1ml PBS, centrifuged for 30 min (14000 rpm at 4°C). The supernatant was collected in aliquots. Equal amount of 50% trichloroacetic acid was added to each 500μl supernatant and incubated over night at 4° C., Supernatant was subsequently centrifuged (30 min, 14000rpm at 4°C) and measured by Infinite M200 plate reader (excitation at 620; emission at 680). Free PBS combined with 50% trichloroacetic acid was regarded as blank, and gradient doses of Evans Blue were measured to draw the standard curve. The results were quantified according to standard curve and presented as (μg of Evans Blue stain)/(g of brain tissue).

Plasmids construction: The 5'-UTR sequence of mouse *CD11b* gene was achieved using Pubmed (http://www.ncbi.nlm.nih.gov/entrez/). The 5'-UTR sequence of mouse *CD11b* gene was further analyzed for potential c-Jun (AP-1) binding sides by using web-based algorithm (NUBIScan and hTFtarget) as we did before [36]. Mouse *CD11b* gene promoter region containing fragment (− 2900 to + 190) was chemically synthesized by Sangon (Shanghai, China) cloned into pGL3-basic vector. All the resulting plasmids were named as pGFs as Fig. 8A shows.

Dual-luciferase reporter assay: Murine brain pericyte cell line MBVP was transiently transfected with reporter plasmids (pGFs) by Lipofectamine 3000 (L3000008, Thermo Fisher). Two hours later the cultured medium was replaced with fresh complete DMEM medium. After 24 hours incubation, NETs-formed or normal medium was added with specific drugs for another 24 hours. Then the cell lysates were collected and luciferase activities were measured by Dual-Luciferase Reporter System (E1910, Promega). The transfection experiments were repeated three times in triplicate, and the transfection efficiency was normalized by dividing firefly luciferase activity to renilla luciferase activity.

Chromatin immunoprecipitation assays: Chromatin immunoprecipitation (ChIP) assays were performed with Pierce™ ChIP assay kit (26157, Thermo Fisher) according to the manufacturer's instructions. The targeted protein-DNA mixture was gathered by PureProteome Magnet (LSKMAGS08, Millipore). Then the final DNA extracts were qPCR or RT-PCR amplified by specific primers (shown in Figure S7). The antibodies against c-Jun and the control IgG were obtained from CST and Beyotime respectively (listed in Table S2).

Neurobehavioral evaluations: *Open-field test*: Mice were tested in a square box (40cm × 40cm × 40cm) for 10 min, and activity was digitally recorded as we did before [37]. Travel distance, mean velocity, and time spent in the center zone were analyzed with Ethovision XT video-tracking software (Noldus Information Technology, Asheville, NC). *Foot-fault test*: The experiments were carried out on an elevated beam (2.5 × 75 cm) raised 76 cm above the floor as previously described [38]. Mice were placed at the beginning of the beam and their movements were manual from the beginning to the end. It was considered an individual foot fault when a mouse paw slipped completely through the beam during its walking. The average foot fault score was calculated from the total steps within 75cm in three separate trials. *Y-maze spontaneous alteration test*: Mice were tested in a Y-shaped maze with three arms at 120° angle from each other, and allowed to explore the three arms freely for 8 min as previously [39]. The number of arm entries and triads were recorded to calculate the percentage of alteration.

Statistical analysis: All data were analyzed and presented by using GraphPad Prism version 5.01 (GraphPad Software). Unpaired two-tailed Student *t* test were evaluated for comparison of treated groups with vehicle controls. For analyzing parameters depending on two factors or more, two-way ANOVA/multivariate analysis of variance (MANOVA) was used with Bonferroni correction. A p value < 0.05 was considered statistically significant. Data in figures were all represented as mean ± SEM with *p < 0.05; **p < 0.01. The number of animals and experimental repeats were marked in the corresponding figure legends.

Results:

Neutrophil infiltration and NETs formation are associated with the CD11b induction in pericyte after TBI.

The leukocyte infiltration of injured brain tissue is an important pathological process during TBI [40, 41]. In TBI patients and mouse model, we observed obvious infiltration of neutrophils in brain tissue within 24 hours (Fig. 1a, CD177; Fig. 1b, CD16). We also found that neutrophils were closely distributed around brain pericytes. This was in consistency with previous report claiming that neutrophil initial infiltration was in close proximity to pericyte [42]. It has been shown that integrin alpha M (CD11b) or intercellular cell adhesion molecule-1 (ICAM-1) is one hallmark of pericyte activation, which are fundamental for pericyte to increase permeability as well as recruit leukocytes [28, 43, 44]. To examine whether neutrophils/ NETs formation gave rise to pericyte activation, we analyzed the relationship between myeloperoxidase (MPO)-DNA binding capacity (a sensitive measurement of NETs formation) of infiltrated neutrophils and CD11b/ICAM-1 expression levels of brain pericytes from 10 TBI patients. Figure 1c&1d showed that there was significant positive correlation between NETs formation and $CD11b^+$ brain pericyte. The correlation ratio between NETs level and ICAM-1 expression showed no statistical difference. In mice, we found similar phenomenon that neutrophils were accumulated around morphologically altered pericyte following TBI, alongside with disrupted BBB structure (Fig. 1e-1g). Moreover, marked with CitH3 and DAPI (combined marker for NETs), we saw decreased expression of pericyte marker PDGFRβ and enhanced level of CitH3 in injured brain tissue (Fig. 1h). Moreover, these website-like DNA structures were not only detectable in injured side, but also in the contralateral side from TBI mice (Fig. 1i&1j). This indicates that neutrophil infiltration and NETs formation are spatially and functionally related with brain pericyte after TBI, in which CD11b expression might be the reason to connect them.

$CD11b^+$ pericyte is endowed with pro-inflammatory profiles.

Since we showed that CD11b expression was a character of NETs-activated pericytes in human, we next confirmed the association between NETs and CD11b expression pericyte in mouse TBI model and investigated the characters of these $CD11b^+$ pericytes. FACS test presented that $CD11b^+$ brain pericyte population was significantly enhanced post TBI (Fig. 2a), which was not obvious in brain endothelial cell (Fig. 2b&2c), indicating that CD11b induction was specific to brain pericyte alongside with NETs formation. After establishing a crucial link between NETs formation and CD11b induction of pericytes, we aimed to investigate the differences between $CD11b^+$ and $CD11b^-$ brain pericytes at a transcriptomic level. To begin with, we harvested brain pericytes ($CD45^-CD13^+$) from brain tissue as previously did [45], and sorted $CD11b^+$ and $CD11b^-$ brain pericytes respectively for further study (Fig. 2d&S1). After culturing these two pericyte subpopulations with complete DMEM medium for 48 hours, $CD11b^+$ pericytes appeared to be round and huddled shape, whilst $CD11b^-$ pericytes were prolonged and stretched (Fig. 2e). This might lead to decreased BBB coverage due to altered morphology of $CD11b^+$ pericyte in damaged brain tissue. Meanwhile, Transwell experiment proved that $CD11b^+$ pericyte were more robust to attract

neutrophils compared to $CD11b^-$ pericytes (Fig. 2f&2g). As shown in Fig. 2h&S2, $CD11b^+$ pericytes exhibited obvious pro-inflammatory characteristics (TNF-α, IL-1β, CCL2/5, CXCL8/10) and BBB disruption (MMP2 and MMP9) examined by high-throughput RNA-sequencing. Realtime-PCR of these sorted cell further confirmed this conclusion (Fig. 2i). These data provide the evidences that $CD11b^+$ pericytes are important contributor during neuroinflammation that can be regarded as activated status post TBI referring to previous study [24, 46–49].

NETs directly induce CD11b expression on pericyte to facilitate increased adhesion and integrity damage in vitro.

Apart from induced NETs formation in brain parenchyma, the circulating neutrophils isolated from TBI mice exhibited higher frequency of NETs formation compared with neutrophil from sham group (Fig. 3a&3b), which was in consistency with Vaibhav K's work [21]. In brain tissues from TBI patient, we confirmed the existence of $CD11b^+$ brain pericyte in parenchyma by immunofluorescence (Fig. 3c). To detect whether NETs directly activated pericyte via regulating CD11b expression, then we stimulated primary brain pericyte or pericyte cell line MVBP with NETs-formed medium at established conditions (obvious effects without strong cytotoxicity according to Figure S3). After cultured with NETs-induced medium for 24 hours, we found that primary pericytes displayed an activated morphological characters of shrunken shape and round cell body (Fig. 3d) as $CD11b^+$ pericyte showed (Fig. 2e). Based on previous study, pericyte activation was associated with various dysfunctions, including decreased tight junction and increased adhesive capacity [24, 50]. To further confirm the association between activation profiles and CD11b induction in pericyte, we utilized murine pericyte cell line (MBVP) to evaluate pericyte functions toward NETs-formed medium. Accordingly, NETs-formed medium significantly changed cell morphology with sparse cell contacts and elongated shapes (Fig. 4a), decreased tight junction (Fig. 4b) and increased neutrophil adhesion (Fig. 4c). Furthermore, NETs-induced medium strongly promoted formation of $CD11b^+$ population (Fig. 4d-4h) and jeopardized integrity (Fig. 4i) accompanied with obvious CD11b induction. All the effects mediated by NETs-induced medium could be reversed by Cl-Amidine (NETs formation inhibitor by decreasing PAD activity), suggesting that NETs formation was associated with pericyte activation alongside with CD11b induction.

Histones are the main components of NETs to drive CD11b induction on pericyte.

As we found that NETs-induced medium significantly changed morphology and functions of pericyte in indirect way, we aimed to investigate what components of NETs-formed medium drive this phenomenon. The effects of neutrophil functions in co-culture system are different depending on direct or indirect cell interactions [51]. The indirect interaction means cell communication occurs through releasing various substances without cell contact. Since we treated pericytes without neutrophil direct contact, these effects were mediated by substances released from neutrophil while forming NETs structure. In Fig. 5a, we collected the cultured medium after removing neutrophils with or without PMA stimulation for proteomics and metabolomics analysis. In proteomic analysis, overall 4098 proteins were identified in these two groups. Proteins with repeatable fold changes > 1.2 or < 0.8 were screened out as differentially

expressed proteins (Fig. 5b&S2). In PMA-stimulated groups, there were 101 up-regulated and 3 down-regulated proteins identified. Of note, histones accounted for 30% of the top up-regulated proteins and other neutrophil intracellular molecules (lactoferrin, complement 3, and metalloproteinase *et al*) were also detectable, which was consistent with reported NETs characters [14]. NETs formation induced by PMA caused dramatic alterations in amino acids too, such as N-acetyl-L-cycteine, L-isoleucine, L-glutamate (Fig. 5c&S3). In order to testify their effects on pericyte, we selected some of these proteins (histones and lactoferrin) or metabolites (N-acetyl-L-cycteine and L-isoleucine) to confirm if they could change CD11b expression *in vitro*. As shown in Fig. 5d-5f, only histones treatments could induce CD11b expression in dose-dependent manner. We did not see obvious alterations (Figure S5) under intended concentrations of lactoferrin, N-acetyl-L-cycteine and L-isoleucine according to previous studies [52, 53]. Recently, several researches have proved that histones released by necrotic cells or NETs were non-negligible factors that drove inflammatory responses [54–56]. The increased level of histones and segmented DNA was highly associated with BBB damage and brain edema [8, 21], supporting our data that histones were the possible components of NETs to drive CD11b induction in brain pericytes.

Dectin-1 is fundamental for pericyte to respond toward histones of NETs in vitro.

After defining histones as the main components of NETs to affect pericyte, we aimed to decipher the possible ways that pericyte might respond to. According to previous study, we converted our attention to C-type lectin receptors (CLRs), a large family of transmembrane receptors that recognized not only fungal moieties, but also histone-related molecules from dead cells [54, 57]. Three types of CLRs are classified based on their molecular structures: type I, type II and soluble type. Of which, Type II CLRs are the main receptors for recognition of histone sequences or histone deacetylase complexes released from disintegrated DNA [54, 58]. Type II CLRs carry a conserved carbohydrate-recognition domain and contain five receptors: Dectin-1, Dectin-2, macrophage-inducible CLR (Mincle), dendritic cell-specific ICAM3-grabbing nonintegrin (DC-SIGN), as well as DC-NK lectin group receptor-1 (DNGR-1) [59]. Based on human protein atlas database, we found that the expressions of type II CLRs in CNS (yellow bars) were relatively low except Dectin-1 and DNGR-1 (Figure S6a). The protein expression and glycosylation level of Dectin-1was obviously upregulated in pericyte cell line with PMA-induced medium or histones (Fig. 6a&S6b). Meanwhile, we found that $CD11b^+$ brain pericyte was armed with higher expression of Dectin-1 compared to $CD11b^+$ population in human samples (Fig. 6b&6c), alongside with increased Dectin-1expression of brain protein after TBI (Figure S6c). This proved that Dectin-1 expression was positively related to CD11b upregulation in brain pericyte. In order to confirm if Dectin-1 was indispensable for CD11b upregulation, the Dectin-1 siRNAs and specific antagonist Laminarin (LAM) were introduced in the following experiments. WB showed that synthetic siRNAs was capable to interfere Dectin-1 protein expression in the presence of NETs-medium and histones (Fig. 6d). Furthermore, antagonizing Dectin-1 by LAM as well as blocking Dectin-1 expression by siRNAs decreased $CD11b^+$ pericyte population and CD11b expression compared to PMA-medium alone (Fig. 6e-6h). This phenomenon was consistent under histones-treated conditions (Fig. 6i-6l), indicating that histones of NETs were crucial factors to induce CD11 expression of brain pericyte in Dectin-1 dependent manner. TEER experiments also confirmed that targeting at Dectin-1

was beneficial for restoring pericyte integrity *in vitro* (Fig. 6m&6n). Here, we show that Dectin-1 antagonist LAM and siRNAs are competent to blunt CD11b expression mediated by NETs medium or histones stimulation, confirming that Dectin-1 is indispensable for pericyte to react toward histones of NETs.

PKC and c-Jun activation mediated by Dectin-1 are responsible for CD11b induction of pericyte during NETs and histones treatments.

Next, we explored the possible signaling pathways mediated by Dectin-1 that were involved in CD11b induction. After reading previous literature, we sorted out that protein kinase Cζ/λ (PKCζ/λ) and transcriptional factor c-Jun were possible molecules post Dectin-1 activation [59]. The levels of phosphorylated PKC (p-PKCζ/λ) and phosphorylated c-Jun (p-c-Jun), activation status of these two molecules, were significantly increased following NETs-formed medium treatment (Fig. 7a). Similar effects were observed in histones treatment group, reiterating the factor that histones were robust to mimic NETs-formed medium. In the presence of Dectin-1 inhibitor LAM and Dectin-1 siRNAs, the phosphorylation levels of PKC and c-Jun dropped dramatically (Fig. 7b&7c), showing that Dectin-1 was essential for PKC and c-Jun activation toward NETs-medium stimulation. PKC specific antagonist GFX as well as c-Jun inhibitor T-5224 were further used to confirm their roles in Dectin-1 mediated pathway stimulated by NETs-formed medium and histones (Fig. 7d). The Realtime-PCR as well as flow experiments both demonstrated that PKC inhibitor or c-Jun inhibitor blunted CD11b expression mediated by Dectin-1 activation (Fig. 7e-7h). Therefore, Dectin-1 contributes to CD11b upregulation expression in brain pericyte toward NETs-formed medium/ histones through the Dectin-1/PKC/c-Jun signaling pathway.

c-Jun directly binds to the promoter sequence of CD11b **to enhance its expression in pericyte.**

Transcription factors (TF) bind to the binding site, upstream to the promoter of target gene, to activate or repress gene expression. The data above presented that c-Jun activation, an important TF, contributed to CD11b induction in pericyte, we'd like to explore if c-Jun could activate *CD11b* transcription by binding to its promoter gene. After searching the possible c-Jun binding sides in *CD11b* promoter gene region by NUBIScan, we screened out two possible sites with the "TGACTCA" motif (Fig. 8a&S7). Subsequently, three luciferase reporters containing different promoter regions of *CD11b* gene were constructed, as well as two mutation luciferase reporters that disrupted binding motif. They were named as pGF1 (-2900 to + 190), pGF2 (-1000 to + 190), pGF3 (-200 to + 190), pGFmut1(-1250 to -1244) and pGFmut2 (-410 to -403) respectively (Fig. 8a).Then luciferase reporter assays showed that the activity of pGF1 and pGF2 was significantly increased in the presence of NETs-formed medium or histones (Fig. 8b), revealing that these two potential binding sites of *CD11b* promoter region were capable to promote *CD11b* gene expression. Of note, the ability of histones to raise *CD11b* promoter activity was relatively low compared to NETs-formed medium (Fig. 8b), indicating that there were other potential components in NETs that induced CD11b expression apart from histones. Moreover, mutating these two side separately both decreased the promoter activity (Fig. 8c), verifying that these two binding sites were required for CD11b induction toward NETs-formed medium or histones treatment in pericyte. Subsequently, ChIP assays further

confirmed that c-Jun could bind to these two *CD11b* promoter regions (-1250 to -1244, -410 to -403) directly (Fig. 8d-8f). Taken together, these results indicate that c-Jun activates CD11b expression by binding to two sites (-1250 to -1244, -410 to -403) in *CD11b* gene promoter region.

Inhibition of NETs formation or Dectin-1 improves brain function recovery after TBI.

Previous study and our results above confirmed that NETs formation and brain pericyte dysfunction contributed to acute TBI pathogenesis [21]. Mechanistically, we proved that histones of NETs facilitated CD11b expression in Dectin-1/PKC/c-Jun pathways, leading to pro-inflammatory profiles and damaged integrity of brain pericyte. It had been shown that blocking Dectin-1 was beneficial for ischemia injury in heart and brain [60, 61]. However, if blocking NETs formation and inhibiting Dectin-1 could decrease pericyte activation, restore BBB integrity and improve TBI long-term outcomes were undetermined. Thus, we explored the effects of Cl-Amidine and LAM at different time points after TBI (Fig. 9a). The mice were treated with or without Cl-Amidine (50mg/kg) and LAM (25 mg/kg and 50mg/kg) intraperitoneally every three days post TBI according to previous study [21, 60]. Administration of Cl-Amidine and LAM significantly reduced BBB permeability and death rate compared with saline group in acute phase (Fig. 9b&9c). These two drugs also improved motor and psychiatric functions in TBI mice after two/four weeks (Fig. 9d-9f). However, we did not see statistically differences in these drug treatment groups at 8 weeks post TBI (Figure S8), which might be the annulled pharmaceutical effect (Figure S8). FACS results also showed that Cl-Amidine and LAM dramatically decreased the amounts of infiltrated neutrophils (Fig. 9g&9h) and $CD11b^+$ brain pericytes in damaged parenchyma (Fig. 9i&9j), which contributed to neurobehavioral improvement. These data provide the evidences that targeting at NETs formation and Dectin-1 are effective to ameliorate pericyte dysfunction and neutrophil infiltration, facilitating neurological recovery after TBI.

Discussion:

In this study, we report that histones of NETs drive pericyte transformation, the important constituent cell of BBB, from a steady state to an active phenotype with high expression of CD11b. The $CD11b^+$ pericytes shrink terminal processes and lower their integrity, leading to decreased vascular coverage and increased permeability of BBB; secrete tremendous inflammatory mediators to attract more circulating leukocytes into brain parenchyma, deteriorating neuroinflammation post TBI. Mechanistically, Dectin-1 on pericytes is responsible for recognizing histones to induce CD11b expression in a PKC-c-Jun dependent manner. Targeting at Dectin-1 and NETs formation significantly pericyte dysfunction and neutrophil infiltration, facilitating neurological recovery after TBI. These data indicate that peripheral blood neutrophil is an essential contributing factor to BBB breakdown by forming NETs, while brain pericyte of BBB is both a target cell and a bridge when neutrophil transmigrates through BBB to exert its pro-inflammatory effect. This builds up cellular and molecular connections between pericyte dysfunction and leukocyte infiltration, which may provide new pathological process after brain injury and novel treatment strategy against TBI.

Pericyte is generally treated as indispensable participant during angiogenesis and microcirculation regulation. Recent years, it has raised increasing interests due to its heterogeneity and plasticity in terms of multiple morphology and protein expression pattern. Brain pericyte is more unique and specific since it has the highest vascular coverage [62] and forms a compact barrier between circulating cell and interstitial space in neurovascular unit [23]. Here, we confirm that $CD11b^+$ brain pericyte is highly induced after TBI, which is characterized with increased ability of leukocyte attraction and damaged integrity. This is also consistent with previous studies that increased expression of G-protein signaling 5 (RGS5), NG2 and CD11b endowed pericytes microglia-like phenotypes under stroke or sterile inflammation conditions [46, 63]. CD11b and ICAM-1 are two important molecules for pericyte to actively instruct immune cells toward inflammatory stimulation [28, 63]. The unapparent correlation between ICAM-1 expression on pericytes and NETs formation does not exclude the possibility that CD11b and ICAM-1could facilitate pericyte activation synergistically in TBI. What's more, activated pericyte mediates neuroinflammation through diverse ways apart from leukocyte recruitment and BBB disruption [25]. The pericyte-endothelium communications [41], ability of fibrotic scarring [64], as well as influence on endocytosis [65] that $CD11b^+$ brain pericyte might exhibit within TBI pathogenesis are desperately needed in the future study. Xie X *et al* demonstrated that targeting at pericyte might be beneficial for patients with TBI, and potentially reduce the risk of developing AD [66]. Here we did not see statistical differences in Y maze between treatment groups (Cl-Amidine, LAM) and saline groups 12 weeks post TBI (Figure S8), even though they decreased the amount of $CD11b^+$ pericyte in acute phase (Fig. 9i). We speculate that these drug's effects may not last that long since we only treated these mice for 2 weeks. Thus, continuous drug administration for longer time post TBI as well other behavioral evaluations about spatial learning and memory function are substantial in the future.

In brain diseases, it has been shown that NETs are associated with cerebral edema, hypoperfusion, BBB damage, neurotoxicity, amyloid β plaque deposition and so forth [19, 21]. However, the detailed mechanisms about how cytotoxic proteins and cytokines carried by NETs perform in brain are still elusive. Here, we have analyzed the component of NETs-formed medium by proteomics and metabolomics methods, confirming histones from NETs are important mediators for brain pericyte activation (Fig. 5). Over time, our knowledge of histones has changed dramatically: from DNA packaging proteins to antimicrobial agents, from inherent factors to self-detrimental agents [56]. Circulating histones from necrotic or dead cells are highly associated with the severity and development of acute inflammatory diseases and ischemia-reperfusion injury [55, 67]. In pre-clinical studies, neutralizing or degrading extracellular histones with specific antibody or heparan sulfates have shown promising effects even though our understandings about histone-induced pathologies are still at the beginning [68]. We build the connection between NETs histones and CD11b induction in brain pericyte, illuminating the possible histone-related molecular mechanism in neuroinflammation. While, it is better to distinguish the differences of histone subtypes upon this phenomenon and determine the functional amino acid sequences that stimulate these responses, providing potential therapeutic and diagnostic targets for TBI and other neuroinflammation-related diseases.

The histones and free nucleic acids from NETs are generally recognized by innate immune system through binding to damage-associated molecular pattern recognition receptors, such as Toll-like receptors (TLRs), cytosolic DNA sensors (CDSs), and Nod-like receptors (NLRs) [69]. Interacting with TLRs and NLRs, Dectin-1 also plays fundamental roles of regulating phagocytosis, ROS and cytokine production in myeloid cells, such as macrophage and neutrophil [61, 70]. Moreover, the recognition for histones [54] and alarmin for neuroinflammation [71, 72] broaden our understanding about Dectin-1 in innate immune system as well as CNS. Latest studies and our data (Figure S6) have showed that Dectin-1 expression is highly enhanced in brain tissue following ischemic injury or TBI, causing overwhelming activation of microglia [60, 73]. This provides the hint that Dectin-1might affect neuroinflammation in multiple ways. Apart from the previous report that Dectin-1 facilitates CD11b activation in neutrophil by forming Vav-PLCγ complex during fungal clearance [74], we for the first time show that Dectin-1 directly induces CD11b expression by promoting c-Jun binding to promoter gene sequence in pericyte (Fig. 8), elucidating the possible molecular mechanism for pericyte activation. However, our data did exclude the possibility that Dectin-1 inhibition could decrease neutrophil infiltration directly apart from pericyte modulation since Dectin-1 contributes neutrophil accumulation based on previous research [75]. Thus, more specific treatment or conditional brain pericyte Dectin-1 knockout will strengthen the conclusion in the future.

Targeting at Dectin-1 and its family receptors were previously focused on infection, and were at the initiation stage of several clinical trials (HBV and fungal infection, oral squamous cell carcinoma treatment *et al*) [76]. Our result that Dectin-1 is involved in NETs-mediated pericyte dysfunction provides the innovative approaches for TBI treatment, broadening the biological effects and therapeutic targets of Dectin-1 in CNS. Also, the price of Dectin-1 inhibitor (LAM) is lower compared to PAD inhibitor (Cl-Amidine) and rhDNase, which might be low-cost and high-reward candidate for TBI patients. There are still some aspects that might limit Dectin-1 applications: inappropriate Dectin-1antagonist administration could induce severe immune deficiency (vulnerable for fungal infection); there is no FDA-approved drugs in clinic targeting at Dectin-1. Further investigations about effective and securable Dectin-1-related drugs are desperately needed.

Conclusions

In conclusion, our data support that activated phenotype ($CD11b^+$) of brain pericyte is highly induced by NETs-associated histones after TBI. Recognition of histones by Dectin-1 in pericyte contributes to CD11b induction in a PKC-c-Jun dependent manner. Targeting at NETs formation and Dectin-1 are efficient for restoring BBB integrity and attenuating neuroinflammation to improve neurological outcomes of TBI.

Abbreviations

BBB: blood-brain barrier; CD11b: integrin alpha M; CitH3: citrullinated histone H3; CLR: C-type lectin receptors; CNS: central nervous system; DC-SIGN: dendritic cell-specific ICAM3-grabbing nonintegrin; DNA: deoxyribonucleic acid; DNGR-1: DC-NK lectin group receptor-1; GCS: glasgow coma scale; ICAM-1: intercellular cell adhesion molecule-1; LAM: Laminarin; Mincle: macrophage-inducible C-type lectin

receptors; MMP: matrix metalloproteinase; NETs: neutrophil extracellular traps; OFT: open-field test; PAD4: peptidylarginine deiminase 4; PDGFRβ: platelet-derived growth factor receptor β; PKC: protein kinase C; PMA: phorbol 12-myritate 13-acetate; SAH: spontaneous intracerebral hemorrhage; TBI: traumatic brain injury.

Declarations

Funding: This work was supported by National Natural Science Foundation of China (32000670, 81771693).

Acknowledgement: Not applicable.

Authors' contributions: Conceptualization, YW.L., L.X. and SS.D.; Methodology, YW.L., J.Z., W.B., M.Z., J.L., N.Y. X.T. and X.C.; Investigation, YW.L., J.Z., L.Z., Y.Z. Y.T. and W.H.; Writing, YW.L. and SS.D.; Review and editing, J.Z., H.W., L.X.; Supervision, H.W., L.X. and SS.D.

Availability of data and material: The datasets and material in this study are available from the corresponding author on reasonable request.

Competing of interest: The authors all declare that they have no competing interest.

Consent for publication: All authors have seen and approved submitting and publishing this paper.

Ethics approval: All studies were approved by the Institutional Research Ethics Committee of Army Medical University, and written informed consent was obtained from each patient's relatives in Department of Neurosurgery, Daping Hospital (Protocol number: ChiCTR-PRC-15006770). All animal procedures were approved by The Institutional Animal Care and Use Committee at Army Medical University.

References

1. Needham EJ, Helmy A, Zanier ER, Jones JL, Coles AJ, Menon DK: **The immunological response to traumatic brain injury.** *J Neuroimmunol* 2019, **332:**112-125.

2. Williams OH, Tallantyre EC, Robertson NP: **Traumatic brain injury: pathophysiology, clinical outcome and treatment.** *J Neurol* 2015, **262:**1394-1396.

3. Werner JK, Stevens RD: **Traumatic brain injury: recent advances in plasticity and regeneration.** *Curr Opin Neurol* 2015, **28:**565-573.

4. Liu YW, Li S, Dai SS: **Neutrophils in traumatic brain injury (TBI): friend or foe?** *J Neuroinflammation* 2018, **15:**146.

5. Liebner S, Dijkhuizen RM, Reiss Y, Plate KH, Agalliu D, Constantin G: **Functional morphology of the blood-brain barrier in health and disease.** *Acta Neuropathol* 2018, **135:**311-336.

6. Kolaczkowska E, Kubes P: **Neutrophil recruitment and function in health and inflammation.** *Nat Rev Immunol* 2013, **13:**159-175.

7. Puy L, Corseaux D, Perbet R, Deramecourt V, Cordonnier C, Bérézowski V: **Neutrophil Extracellular Traps (NETs) Infiltrate Haematoma And Surrounding Brain Tissue after Intracerebral Haemorrhage: a Post-Mortem Study.** *Neuropathol Appl Neurobiol* 2021.

8. Kang L, Yu H: **Neutrophil extracellular traps released by neutrophils impair revascularization and vascular remodeling after stroke.** 2020, **11:**2488.

9. Shaftel SS, Carlson TJ, Olschowka JA, Kyrkanides S, Matousek SB, O'Banion MK: **Chronic interleukin-1β expression in mouse brain leads to leukocyte infiltration and neutrophil-independent blood–brain barrier permeability without overt neurodegeneration.** *Journal of Neuroscience* 2007, **27:**9301-9309.

10. Shi Y, Zhang L, Pu H, Mao L, Hu X, Jiang X: **Rapid endothelial cytoskeletal reorganization enables early blood-brain barrier disruption and long-term ischaemic reperfusion brain injury.** 2016, **7:**10523.

11. Takei H, Araki A, Watanabe H, Ichinose A, Sendo F: **Rapid killing of human neutrophils by the potent activator phorbol 12-myristate 13-acetate (PMA) accompanied by changes different from typical apoptosis or necrosis.** *J Leukoc Biol* 1996, **59:**229-240.

12. Brinkmann V, Reichard U, Goosmann C, Fauler B, Uhlemann Y, Weiss DS, Weinrauch Y, Zychlinsky A: **Neutrophil extracellular traps kill bacteria.** *Science* 2004, **303:**1532-1535.

13. Yipp BG, Kubes P: **NETosis: how vital is it?** *Blood* 2013, **122:**2784-2794.

14. Tan C, Aziz M, Wang P: **The vitals of NETs.** *J Leukoc Biol* 2020.

15. Song W, Ye J, Pan N, Tan C, Herrmann M: **Neutrophil Extracellular Traps Tied to Rheumatoid Arthritis: Points to Ponder.** *Front Immunol* 2020, **11:**578129.

16. Keshari RS, Jyoti A, Dubey M, Kothari N, Kohli M, Bogra J, Barthwal MK, Dikshit M: **Cytokines induced neutrophil extracellular traps formation: implication for the inflammatory disease condition.** *PLoS One* 2012, **7:**e48111.

17. Shinde-Jadhav S, Mansure JJ, Rayes RF, Marcq G: **Role of neutrophil extracellular traps in radiation resistance of invasive bladder cancer.** 2021, **12:**2776.

18. Cedervall J, Zhang Y, Huang H, Zhang L, Femel J, Dimberg A, Olsson AK: **Neutrophil Extracellular Traps Accumulate in Peripheral Blood Vessels and Compromise Organ Function in Tumor-Bearing**

Animals. *Cancer Res* 2015, **75:**2653-2662.

19. Manda-Handzlik A, Demkow U: **The Brain Entangled: The Contribution of Neutrophil Extracellular Traps to the Diseases of the Central Nervous System.** *Cells* 2019, **8**.

20. Zeng H, Fu X, Cai J, Sun C, Yu M, Peng Y, Zhuang J, Chen J, Chen H, Yu Q, et al: **Neutrophil Extracellular Traps may be a Potential Target for Treating Early Brain Injury in Subarachnoid Hemorrhage.** 2021.

21. Vaibhav K, Braun M, Alverson K, Khodadadi H, Kutiyanawalla A, Ward A, Banerjee C, Sparks T, Malik A, Rashid MH: **Neutrophil extracellular traps exacerbate neurological deficits after traumatic brain injury.** *Sci Adv* 2020, **6:**eaax8847.

22. Yipp BG, Petri B, Salina D, Jenne CN, Scott BN, Zbytnuik LD, Pittman K, Asaduzzaman M, Wu K, Meijndert HC, et al: **Infection-induced NETosis is a dynamic process involving neutrophil multitasking in vivo.** *Nat Med* 2012, **18:**1386-1393.

23. Sweeney MD, Ayyadurai S, Zlokovic BV: **Pericytes of the neurovascular unit: key functions and signaling pathways.** 2016, **19:**771-783.

24. Smyth LCD, Rustenhoven J, Park TI, Schweder P, Jansson D, Heppner PA, O'Carroll SJ, Mee EW, Faull RLM, Curtis M, Dragunow M: **Unique and shared inflammatory profiles of human brain endothelia and pericytes.** *J Neuroinflammation* 2018, **15:**138.

25. Rustenhoven J, Jansson D, Smyth LC, Dragunow M: **Brain Pericytes As Mediators of Neuroinflammation.** *Trends Pharmacol Sci* 2017, **38:**291-304.

26. Birbrair A: **Pericyte Biology: Development, Homeostasis, and Disease.** *Adv Exp Med Biol* 2018, **1109:**1-3.

27. Hyun YM, Choe YH: **LFA-1 (CD11a/CD18) and Mac-1 (CD11b/CD18) distinctly regulate neutrophil extravasation through hotspots I and II.** 2019, **51:**1-13.

28. Proebstl D, Voisin MB, Woodfin A, Whiteford J, D'Acquisto F, Jones GE, Rowe D, Nourshargh S: **Pericytes support neutrophil subendothelial cell crawling and breaching of venular walls in vivo.** *J Exp Med* 2012, **209:**1219-1234.

29. Yang T, Liu Y-W, Zhao L, Wang H, Yang N, Dai S-S, He F: **Metabotropic glutamate receptor 5 deficiency inhibits neutrophil infiltration after traumatic brain injury in mice.** *Scientific Reports* 2017, **7:**9998.

30. Liu YW, Yang T, Zhao L, Ni Z, Yang N, He F, Dai SS: **Activation of Adenosine 2A receptor inhibits neutrophil apoptosis in an autophagy-dependent manner in mice with systemic inflammatory response syndrome.** *Sci Rep* 2016, **6:**33614.

31. Hørlyck S, Helms HCC, Brodin B: **Culture of Brain Capillary Pericytes for Cytosolic Calcium Measurements and Calcium Imaging Studies.** *J Vis Exp* 2020.

32. Crouch EE, Doetsch F: **FACS isolation of endothelial cells and pericytes from mouse brain microregions.** 2018, **13:**738-751.

33. Rathmann D, Rijntjes E, Lietzow J, Köhrle J: **Quantitative Analysis of Thyroid Hormone Metabolites in Cell Culture Samples Using LC-MS/MS.** *Eur Thyroid J* 2015, **4:**51-58.

34. Wang Z, Liu F, Ye S, Jiang P, Yu X, Xu J, Du X, Ma L, Cao H, Yuan C, et al: **Plasma proteome profiling of high-altitude polycythemia using TMT-based quantitative proteomics approach.** *J Proteomics* 2019, **194:**60-69.

35. Devraj G, Guérit S, Seele J, Spitzer D, Macas J, Khel MI, Heidemann R, Braczynski AK, Ballhorn W, Günther S, et al: **HIF-1α is involved in blood-brain barrier dysfunction and paracellular migration of bacteria in pneumococcal meningitis.** 2020, **140:**183-208.

36. Zhao L, Liu YW, Yang T, Gan L, Yang N, Dai SS, He F: **The mutual regulation between miR-214 and A2AR signaling plays an important role in inflammatory response.** *Cell Signal* 2015, **27:**2026-2034.

37. Liu YW, Zhao L, Zhou M, Wang H, Yang N, Dai SS: **Transplantation with mGluR5 deficiency bone marrow displays antidepressant-like effect in C57BL/6J mice.** *Brain Behav Immun* 2019.

38. Bajwa NM, Lee JB, Halavi S, Hartman RE, Obenaus A: **Repeated isoflurane in adult male mice leads to acute and persistent motor decrements with long-term modifications in corpus callosum microstructural integrity.** 2019, **97:**332-345.

39. Alegre-Zurano L, Martín-Sánchez A, Valverde O: **Behavioural and molecular effects of cannabidiolic acid in mice.** *Life Sci* 2020, **259:**118271.

40. Obermeier B, Daneman R, Ransohoff RM: **Development, maintenance and disruption of the blood-brain barrier.** *Nat Med* 2013, **19:**1584-1596.

41. Bhowmick S, D'Mello V, Caruso D, Wallerstein A, Abdul-Muneer PM: **Impairment of pericyte-endothelium crosstalk leads to blood-brain barrier dysfunction following traumatic brain injury.** *Exp Neurol* 2019, **317:**260-270.

42. Liu R, Lauridsen HM: **IL-17 Promotes Neutrophil-Mediated Immunity by Activating Microvascular Pericytes and Not Endothelium.** 2016, **197:**2400-2408.

43. Stark K, Eckart A, Haidari S, Tirniceriu A, Lorenz M, von Bruhl ML, Gartner F, Khandoga AG, Legate KR, Pless R, et al: **Capillary and arteriolar pericytes attract innate leukocytes exiting through venules and 'instruct' them with pattern-recognition and motility programs.** *Nat Immunol* 2013, **14:**41-51.

44. Wang S, Cao C, Chen Z, Bankaitis V, Tzima E, Sheibani N, Burridge K: **Pericytes regulate vascular basement membrane remodeling and govern neutrophil extravasation during inflammation.** *PLoS One* 2012, **7:**e45499.

45. Crouch EE, Doetsch F: **FACS isolation of endothelial cells and pericytes from mouse brain microregions.** *Nat Protoc* 2018, **13:**738-751.

46. Özen I, Deierborg T, Miharada K, Padel T, Englund E, Genové G, Paul G: **Brain pericytes acquire a microglial phenotype after stroke.** *Acta Neuropathol* 2014, **128:**381-396.

47. Sakai K, Takata F, Yamanaka G, Yasunaga M, Hashiguchi K, Tominaga K, Itoh K, Kataoka Y, Yamauchi A, Dohgu S: **Reactive pericytes in early phase are involved in glial activation and late-onset hypersusceptibility to pilocarpine-induced seizures in traumatic brain injury model mice.** *J Pharmacol Sci* 2021, **145:**155-165.

48. Cai W, Liu H, Zhao J, Chen LY, Chen J, Lu Z, Hu X: **Pericytes in Brain Injury and Repair After Ischemic Stroke.** *Transl Stroke Res* 2017, **8:**107-121.

49. Sakuma R, Kawahara M, Nakano-Doi A, Takahashi A, Tanaka Y, Narita A, Kuwahara-Otani S, Hayakawa T, Yagi H, Matsuyama T, Nakagomi T: **Brain pericytes serve as microglia-generating multipotent vascular stem cells following ischemic stroke.** *J Neuroinflammation* 2016, **13:**57.

50. Armulik A, Genové G, Mäe M, Nisancioglu MH, Wallgard E, Niaudet C, He L, Norlin J, Lindblom P, Strittmatter K: **Pericytes regulate the blood-brain barrier.** *Nature* 2010, **468:**557.

51. Xie L, Poteet EC, Li W, Scott AE, Liu R, Wen Y, Ghorpade A, Simpkins JW, Yang SH: **Modulation of polymorphonuclear neutrophil functions by astrocytes.** *J Neuroinflammation* 2010, **7:**53.

52. Mao X, Qi S, Yu B, He J, Yu J, Chen D: **Zn(2+) and L-isoleucine induce the expressions of porcine β-defensins in IPEC-J2 cells.** *Mol Biol Rep* 2013, **40:**1547-1552.

53. Huang HC, Lin H, Huang MC: **Lactoferrin promotes hair growth in mice and increases dermal papilla cell proliferation through Erk/Akt and Wnt signaling pathways.** *Arch Dermatol Res* 2019, **311:**411-420.

54. Lai JJ, Cruz FM, Rock KL: **Immune Sensing of Cell Death through Recognition of Histone Sequences by C-Type Lectin-Receptor-2d Causes Inflammation and Tissue Injury.** *Immunity* 2020, **52:**123-135.e126.

55. Shah M, Yellon DM, Davidson SM: **The Role of Extracellular DNA and Histones in Ischaemia-Reperfusion Injury of the Myocardium.** 2020, **34:**123-131.

56. Moiana M, Aranda F, de Larrañaga G: **A focus on the roles of histones in health and diseases.** *Clin Biochem* 2021.

57. Drouin M, Saenz J, Chiffoleau E: **C-Type Lectin-Like Receptors: Head or Tail in Cell Death Immunity.** *Front Immunol* 2020, **11:**251.

58. Patin EC, Orr SJ, Schaible UE: **Macrophage Inducible C-Type Lectin As a Multifunctional Player in Immunity.** *Front Immunol* 2017, **8:**861.

59. Nikolakopoulou C, Willment JA, Brown GD: **C-Type Lectin Receptors in Antifungal Immunity.** *Adv Exp Med Biol* 2020, **1204:**1-30.

60. Ye XC, Hao Q, Ma WJ, Zhao QC, Wang WW, Yin HH, Zhang T, Wang M, Zan K, Yang XX, et al: **Dectin-1/Syk signaling triggers neuroinflammation after ischemic stroke in mice.** *J Neuroinflammation* 2020, **17:**17.

61. Fan Q, Tao R, Zhang H, Xie H, Lu L, Wang T, Su M, Hu J, Zhang Q, Chen Q, et al: **Dectin-1 Contributes to Myocardial Ischemia/Reperfusion Injury by Regulating Macrophage Polarization and Neutrophil Infiltration.** *Circulation* 2019, **139:**663-678.

62. Kim ND, Luster AD: **The role of tissue resident cells in neutrophil recruitment.** *Trends Immunol* 2015, **36:**547-555.

63. Stark K, Eckart A, Haidari S, Tirniceriu A, Lorenz M, von Brühl ML, Gärtner F, Khandoga AG, Legate KR, Pless R, et al: **Capillary and arteriolar pericytes attract innate leukocytes exiting through venules and 'instruct' them with pattern-recognition and motility programs.** *Nat Immunol* 2013, **14:**41-51.

64. Hesp ZC, Yoseph RY, Suzuki R, Jukkola P, Wilson C: **Proliferating NG2-Cell-Dependent Angiogenesis and Scar Formation Alter Axon Growth and Functional Recovery After Spinal Cord Injury in Mice.** 2018, **38:**1366-1382.

65. Ojo J, Eisenbaum M, Shackleton B, Lynch C, Joshi U, Saltiel N, Pearson A, Ringland C, Paris D, Mouzon B, et al: **Mural cell dysfunction leads to altered cerebrovascular tau uptake following repetitive head trauma.** *Neurobiol Dis* 2021, **150:**105237.

66. Wu Y, Wu H, Zeng J, Pluimer B, Dong S, Xie X, Guo X, Ge T, Liang X, Feng S, et al: **Mild traumatic brain injury induces microvascular injury and accelerates Alzheimer-like pathogenesis in mice.** 2021, **9:**74.

67. Szatmary P, Huang W, Criddle D, Tepikin A, Sutton R: **Biology, role and therapeutic potential of circulating histones in acute inflammatory disorders.** *J Cell Mol Med* 2018, **22:**4617-4629.

68. Karki P, Birukov KG, Birukova AA: **Extracellular histones in lung dysfunction: a new biomarker and therapeutic target?** *Pulm Circ* 2020, **10:**2045894020965357.

69. Gong T, Liu L, Jiang W, Zhou R: **DAMP-sensing receptors in sterile inflammation and inflammatory diseases.** 2020, **20:**95-112.

70. Underhill DM: **Collaboration between the innate immune receptors dectin-1, TLRs, and Nods.** *Immunol Rev* 2007, **219:**75-87.

71. Baldwin KT, Carbajal KS, Segal BM, Giger RJ: **Neuroinflammation triggered by β-glucan/dectin-1 signaling enables CNS axon regeneration.** *Proceedings of the National Academy of Sciences* 2015, **112:**2581-2586.

72. Gensel JC, Wang Y, Guan Z, Beckwith KA, Braun KJ, Wei P, McTigue DM, Popovich PG: **Toll-Like Receptors and Dectin-1, a C-Type Lectin Receptor, Trigger Divergent Functions in CNS Macrophages.** *The Journal of Neuroscience* 2015, **35:**9966-9976.

73. Fu X, Zeng H, Zhao J, Zhou G, Zhou H, Zhuang J, Xu C, Li J, Peng Y, Cao Y, et al: **Inhibition of Dectin-1 Ameliorates Neuroinflammation by Regulating Microglia/Macrophage Phenotype After Intracerebral Hemorrhage in Mice.** 2021.

74. Li X, Utomo A, Cullere X, Choi MM, Milner DA, Jr., Venkatesh D, Yun SH, Mayadas TN: **The β-glucan receptor Dectin-1 activates the integrin Mac-1 in neutrophils via Vav protein signaling to promote Candida albicans clearance.** *Cell Host Microbe* 2011, **10:**603-615.

75. Yamaguchi K, Kanno E, Tanno H, Sasaki A, Kitai Y, Miura T, Takagi N, Shoji M, Kasamatsu J, Sato K, et al: **Distinct Roles for Dectin-1 and Dectin-2 in Skin Wound Healing and Neutrophilic Inflammatory Responses.** *J Invest Dermatol* 2021, **141:**164-176.e168.

76. Tone K, Stappers MHT: **C-type lectin receptors of the Dectin-1 cluster: Physiological roles and involvement in disease.** 2019, **49:**2127-2133.

Figures

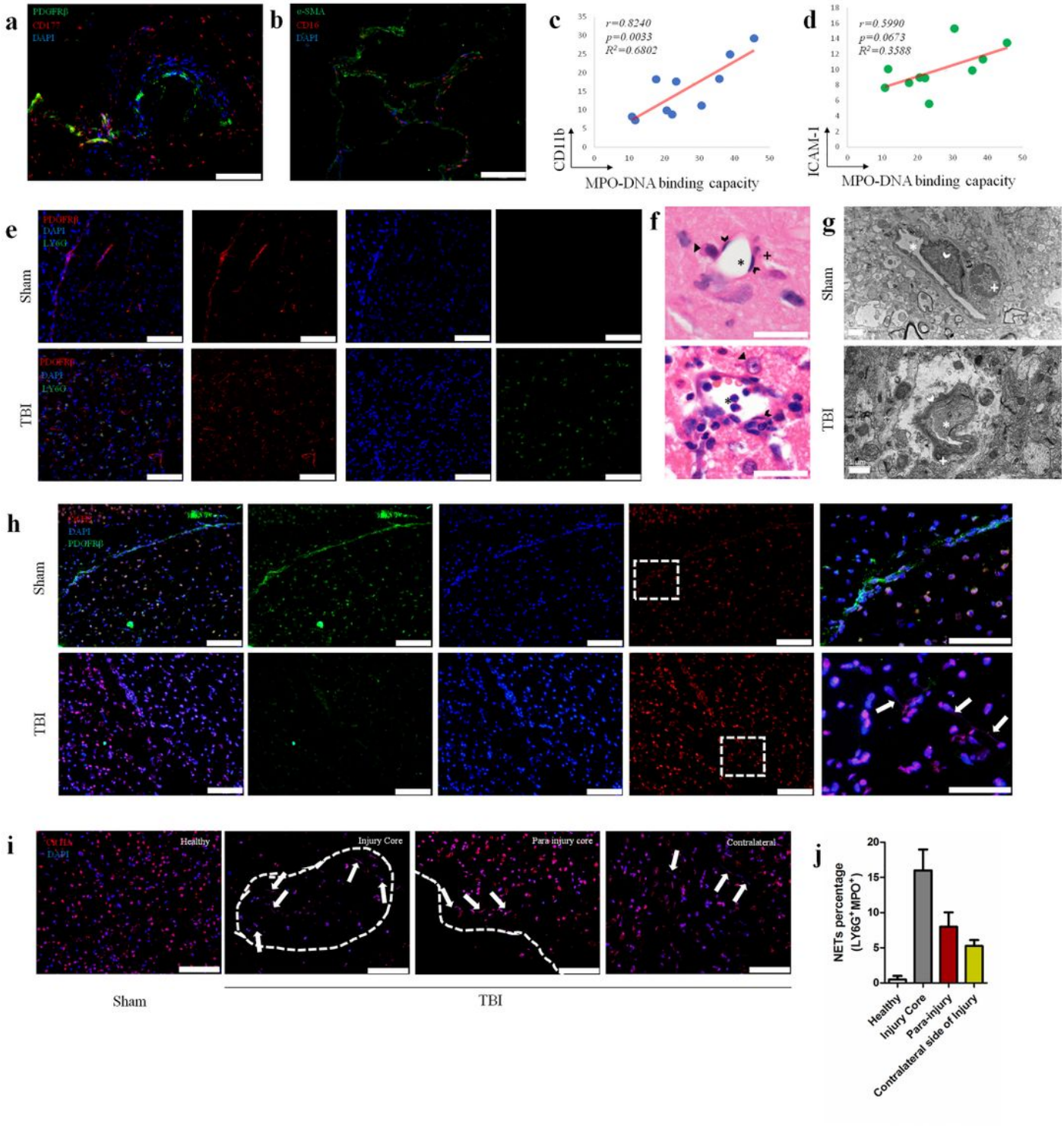

Figure 1

Neutrophil infiltration, NETs formation and pericyte dysfunction post TBI. a&b Immunostaining of pericyte (PDGFRβ, α-SMA) and neutrophil (CD177, CD16) in brain tissues from TBI patients. White scale bar 100μm. c&d Correlation analysis between NETs formation (MPO-DNA binding capacity) and CD11b/ICAM-1 expression level of pericyte isolated from injured brain tissues (n=10). Pearson's correlation coefficient (r), effective R square (R2) and p value are shown as insets. e Immunofluorescence

of pericyte (PDGFRβ) and infiltrated neutrophil (LY6G) in mouse brain at 24 hours after TBI insults. Sham represents the mouse went through the same surgical procedures without impact as control. White scale bar, 100μm. f&g HE stain (f) and TEM (g) of mouse brain vascular unit at 24 hours after TBI. The asterisk (*) represents lumen, the arrow (>) represents endothelial cell, the triangle (Δ) represents astrocyte and the cross (+) represents pericyte. White bar in HE (f) 50μm. White bar in TEM (g) 1μm. h Detection of NETs formation (Cit H3 combined DAPI) and pericyte (PDGFRβ). White arrows point the NETs characters of web-like nucleic acids (patulous and elongated shape of DAPI) and enhanced citrullinated histone 3 (Cit H3) in brain tissue at 24 hours after TBI. White scale bar, 100μm. i Morphology of NETs formation in different brain regions at 24 hours after TBI. White scale bar, 100μm. j FACS analysis of NETs formation (LY6G+MPO+) rates in different brain regions of (i). Each bar represents 5 individual experiments. Cell nuclei were all stained with DAPI.

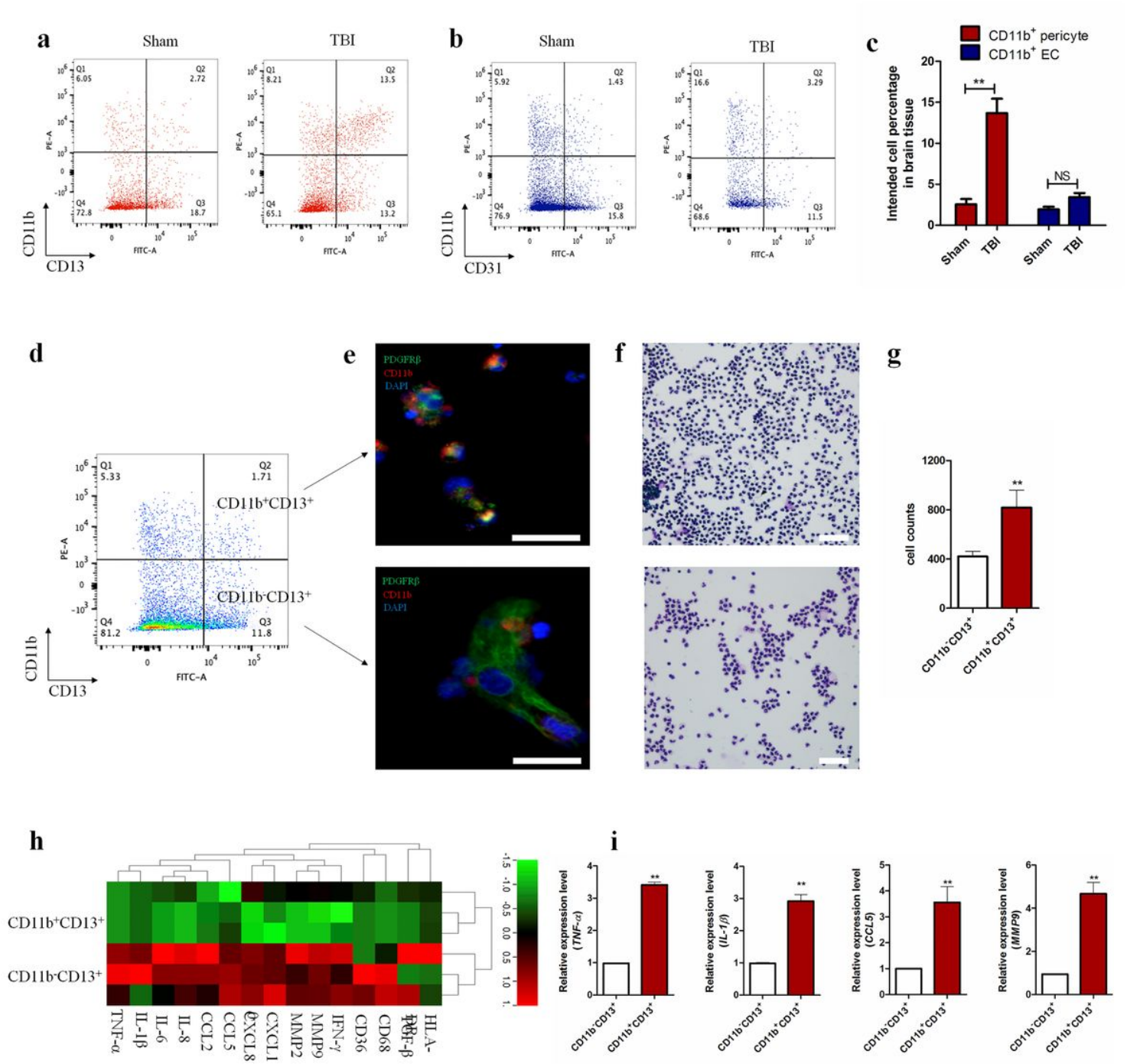

Figure 2

Morphological, functional and molecular features of CD11b positive pericyte after TBI. a&b FACS scatter plots are presented to show CD11b expression of pericyte (a) and endothelial cell (b) in mouse pericontusional brain tissues at 24 hours after TBI. c Qualified data of a&b, Sham and TBI groups both contain 5 mice. d Diagram of brain pericyte (CD13) combined with CD11b expression, CD11b+CD13+(Q2) and CD11b-CD13+(Q3) were sorted for the following experiments. e Morphology of different pericyte subpopulations. After culturing for 2 days with DMEM, the sorted cells (CD11b+CD13+ and CD11b-

CD13+) were stained with CD11b (AlexaFlour 555 tagged) and PDGFRβ (AlexaFlour 488 tagged) for immunofluorescence analysis. White bar represents 10μm. f&g Recruiting capacity of different pericyte subpopulations. The sorted cells were also coated in lower chamber of Transwell Niche for mouse neutrophil chemotaxis experiment. The migrated neutrophils were harvested, stained with Wright Giemsa compound (f) and counted for statistical analysis (g). White bar represents 100μm. Each group contains three separate experiments. h RNA-sequencing data of sorted cells (CD11b+CD13+ and CD11b-CD13+) isolated from mouse injured brain tissues (n=3) at 24 hours after TBI. i qRT-PCR validation of screened-out genes with interests (TNF-α, IL-1β, CCL5 and MMP9) from mouse brain pericyte subpopulations at 24 hours after TBI. CD11b-CD13+ were set as control group. Data are shown as mean±SEM, presented for 3 individual experiments and analyzed by two-tailed unpaired Student's t test. **p<0.01, NS no statistical difference.

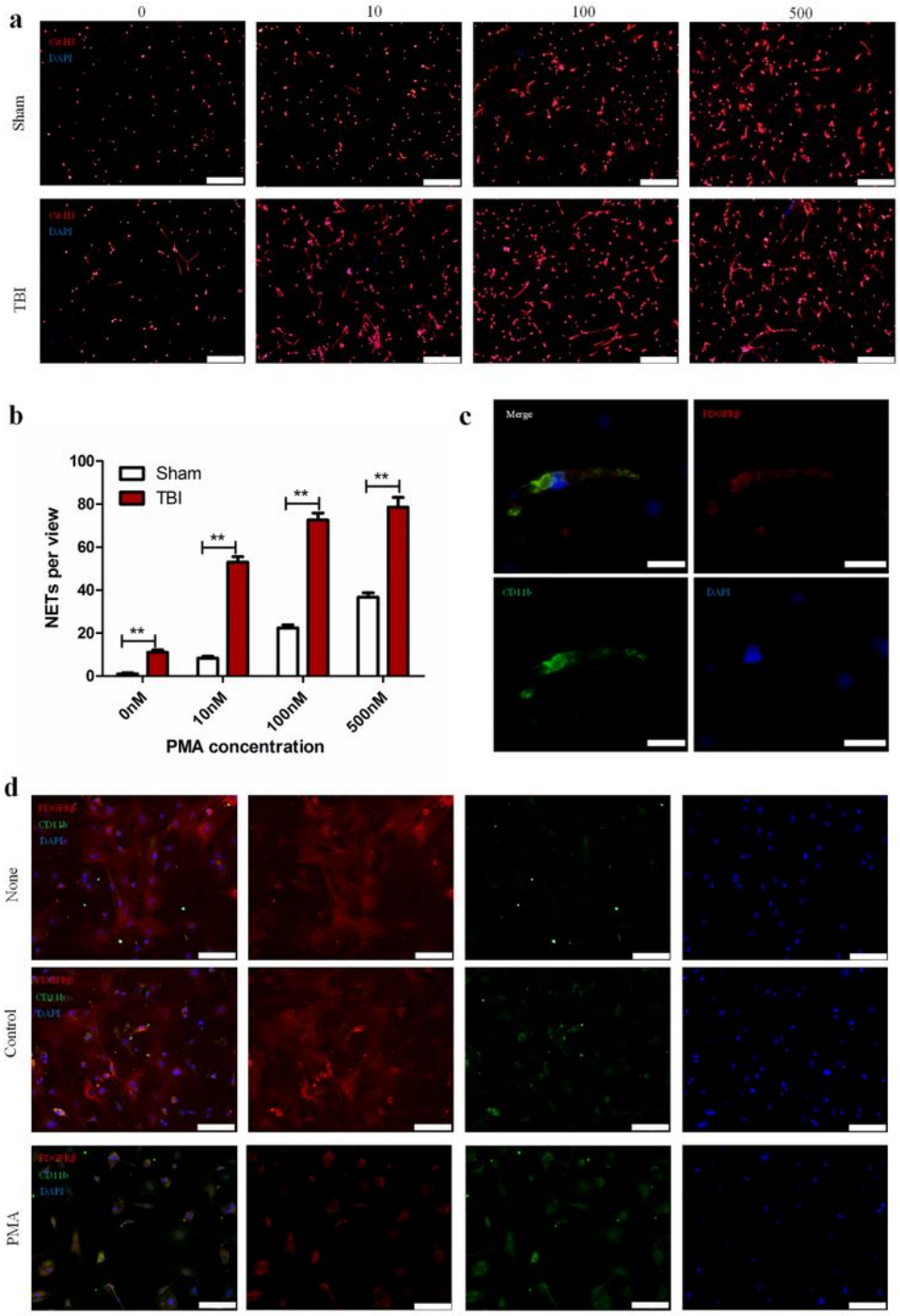

Figure 3

NETs formation and its impact on primary isolated brain pericyte after TBI. a Analysis of NETs formation from peripheral blood. The neutrophils were collected from peripheral blood of Sham and TBI mice at 24 hours post injury. Then the cells were treated with gradient concentrations of PMA (10 ng/ml, 100 ng/ml, 500 ng/ml) for 6 hours and stained with Cit H3 and DAPI. White scale bar 200μm. b Qualification of NETs formation rate in (a). The NETs structures were counted from 5-10 random field in each group. **p<0.01. c

Immunofluorescence of pericyte (red) that expressing CD11b (green) in injured brain from TBI patient. White scale bar 10μm. d Impact on primary-isolated brain pericyte mediated by NETs-formed medium (detailed process is described in method). The freshly-isolated and cultured mouse brain pericyte was cultured with or without NETs-formed medium. None means pericyte was cultured under normal condition. The same amounts of neutrophils were treated with or without PMA (100ng/ml) for 6 hours, then the medium was collected (detailed in method neutrophil isolation and treatment) as PMA and control group. Then the collected medium was mixed with normal culture medium by the ratio of 1:3 and incubated with primary pericyte cells for 24 hours. Subsequently, the cells were fixed and stained with PDGFRβ (red) and CD11b (green). Cell nuclei were all stained with DAPI. White scale bar 100μm.

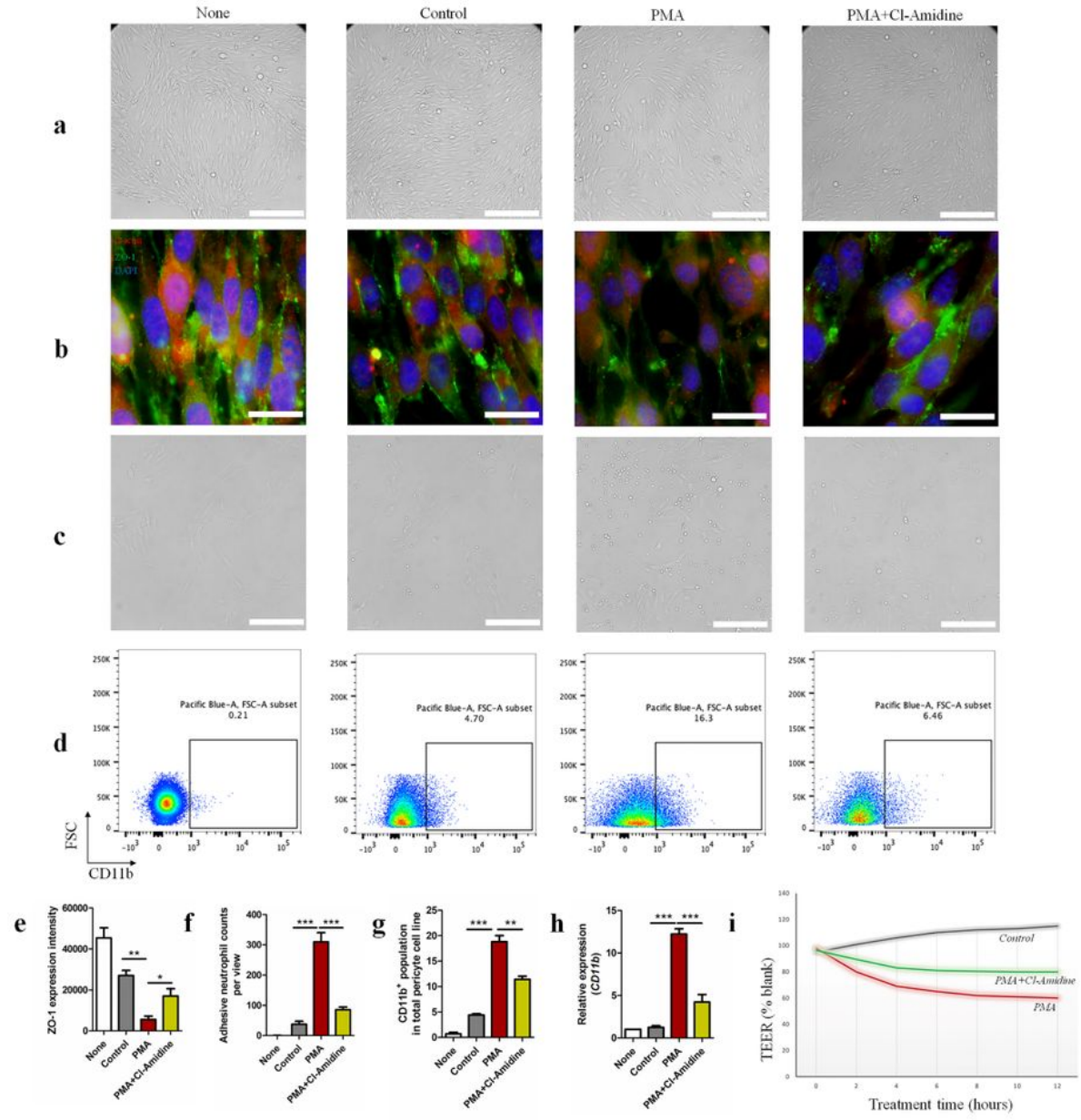

Figure 4

Effects of NETs-formed medium on pericyte cell line MBVP. Murine brain pericyte cell line MBVP was incubated with intended mixed-culture medium as described above for 48 hours. None means normal medium, control means neutrophil without PMA stimulation, PMA means NETs formation stimulated by PMA (100ng/ml), PMA+Cl-Amidine means PMA stimulation (100ng/ml) combined with NETs inhibitor Cl-Amidine (10μM). a Morphological features of MBVP in different groups observed by light microscope.

White scale bar, 100μm. b Immunostaining of tight junction protein (ZO-1, green) and skeleton protein (β-actin, red). White scale bar, 10μm. c Neutrophil adhesion test of MBVP. After 48 hours incubation with intended medium, MBVP was cocultured with 104 freshly-isolated neutrophil in each 6-well plate for 2 hours. Then the coculture plates were washed with PBS for 5 times and observed under light microscope. The big outstretched shapes with low cell diopter were MBVPs, the small round shape with high cell diopter were neutrophils. White scale bar 100μm. d Percentage of CD11b+ MBVP analyzed by FACSs. e Quantification of ZO-1 expression fluorescence intensity in (b). f Quantification of adhesive neutrophils in (c). g Quantification of CD11b+ MBVP population in (d). h Realtime-PCR analysis of CD11b relative levels in different groups. i Representative graph of continuous TEER values of MBVP incubated with intended culture medium. Data are shown as mean±SEM, presented for 3 individual experiments and analyzed by ANOVA. *$p<0.05$, **$p<0.01$, ***$p<0.001$.

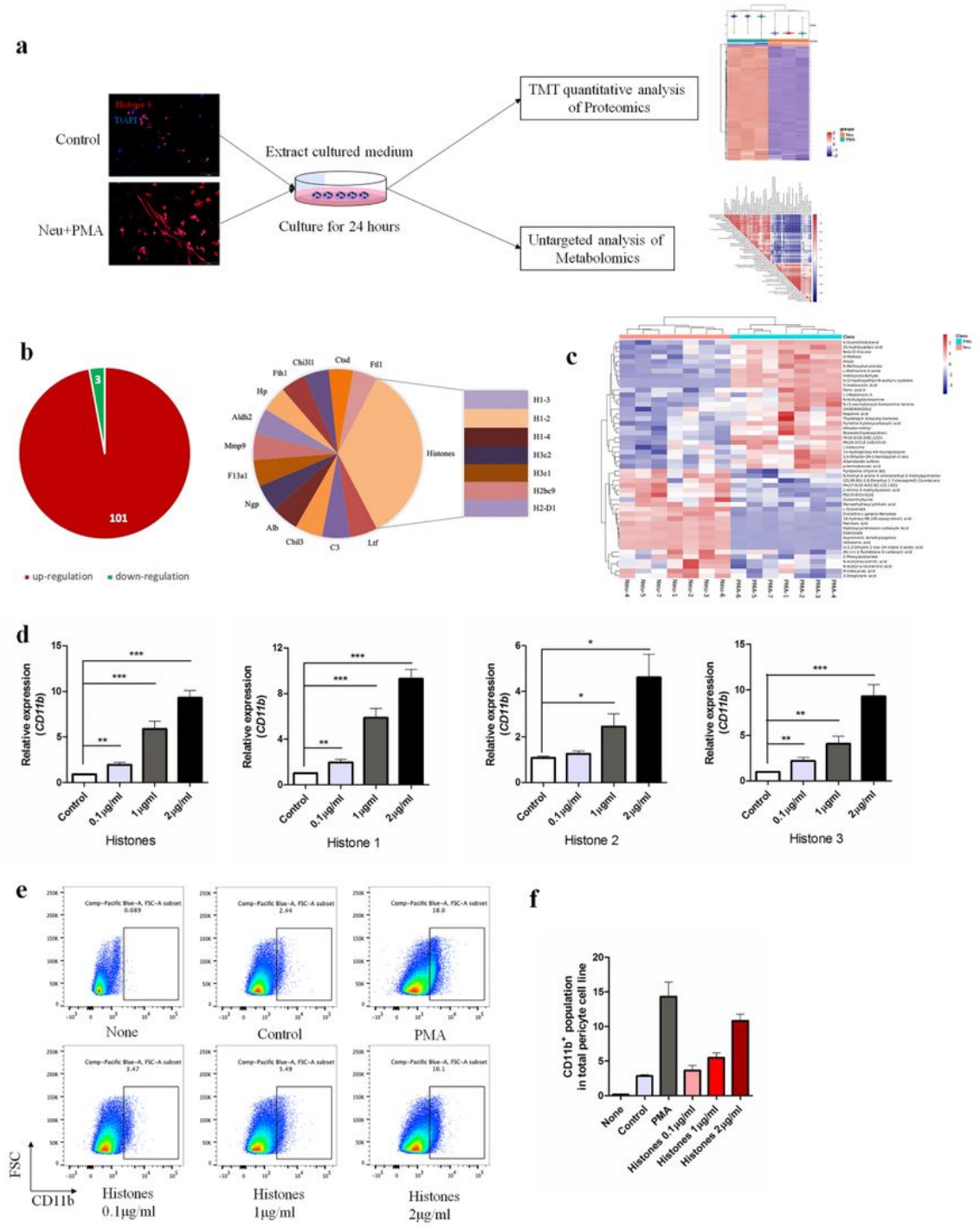

Figure 5

Analysis of functional components from NETs-formed medium affecting pericyte phenotype. a Workflow for proteomics and metabolomics comparisons between NETs-formed medium (PMA) and control medium (neutrophils without PMA stimulation). Proteomics n=3 for each group. Metabolomis n=7 for each group. b Pie chart of differential proteins and top 20 up-regulated proteins in NETs-formed medium. Changes greater than 1.5-fold and $p < 0.05$ were considered significantly differential. c Hierarchical

clustering of differential metabolites in NETs-formed medium. Differential molecules repeatedly consistent in the same group with p value<0.05 were screened out and highlighted in red (up-regulated) and blue (down-regulated). d Realtime-PCR analysis of CD11b relative expression in MBVP stimulated with indicated recombinant mouse histone peptides for 24 hours. Histones represent mixture of histone 1, histone 2 and histone 3 at the ration of 1:1:1. e Percentage of CD11b+ MBVP analyzed by FACS after incubation for 48 hours under indicated conditions. The groups of None, Control and PMA were detailed described in Figure 3. f Quantification of CD11b+ MBVP population in (e). Data are shown as mean±SEM, presented for 3 individual experiments and analyzed by One-way ANOVA. *p<0.05, **p<0.01, ***p<0.001.

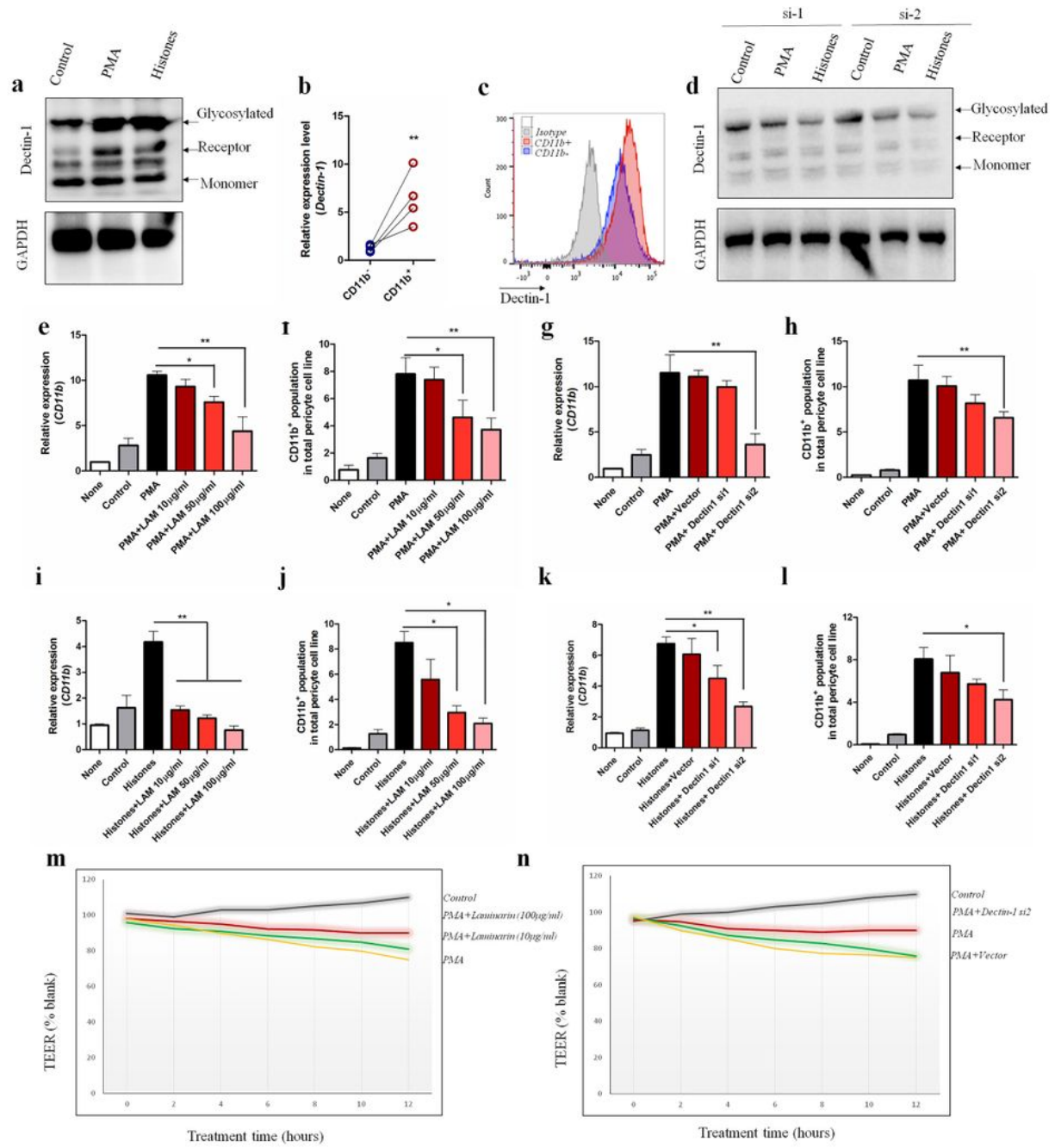

Figure 6

Dectin-1 in pericyte recognized histones from NETs. Pretreated medium: Control means neutrophil without PMA stimulation, PMA means NETs formation stimulated by PMA (100ng/ml), Histones means mixed purified histone peptides (H1, H2 and H3) were dissolved at 2μg/ml. a WB analysis of Detin-1expression in pericyte cell line MBVP incubated with mixed-culture medium for 48 hours. The pre-treated medium was mixed with normal culture medium at the ratio of 1:3 as described above. b Relative

expression of Dectin-1 mRNA in CD11b- and CD11b+ brain pericyte. The mouse brain pericyte subpopulations were sorted as Figure 2 showed. Individual experiments were performed 4 times. c FACS analysis of Dectin-1 expression in human brain pericyte isolated from TBI patient. Isotype means cells were stained with secondary antibody without Dectin-1 antibody. CD11b- human brain pericyte (CD45-CD13+CD11b-, blue) and CD11b+ human brain pericyte (CD45-CD13+CD11b+, red) were further gated to analyze the expression of Dectin-1. d Protein expression of Detin-1 expression in MBVP after transfecting Dectin-1 siRNAs (si-1, si-2). e&f Relative CD11b mRNA expression and CD11b+ population of MBVP under intended conditions for 48 hours. Dectin-1 antagonist was introduced at indicated concentrations. g&h Relative CD11b mRNA expression and CD11b+ population of MBVP after transfecting Dectin-1 siRNAs for 48 hours. Vector means adding transfection solution without siRNAs. i&j Relative CD11b mRNA expression and CD11b+ population of MBVP stimulated with Histones (2μg/ml) in the presence of gradient doses of Dectin-1 antagonist for 48 hours. k&l Relative CD11b mRNA expression and CD11b+ population of MBVP stimulated with Histones (2μg/ml) after transfecting Dectin-1 siRNAs for 48 hours. Vector means adding transfection solution without siRNAs. Data of graphs (e-l) are shown as mean±SEM, presented for 3 individual experiments and analyzed by One-way ANOVA. *$p<0.05$, **$p<0.01$. m&n Representative graph of continuous TEER values of MBVP mediated by Dectin-1 antagonist (m) or Dectin-1 interference (n).

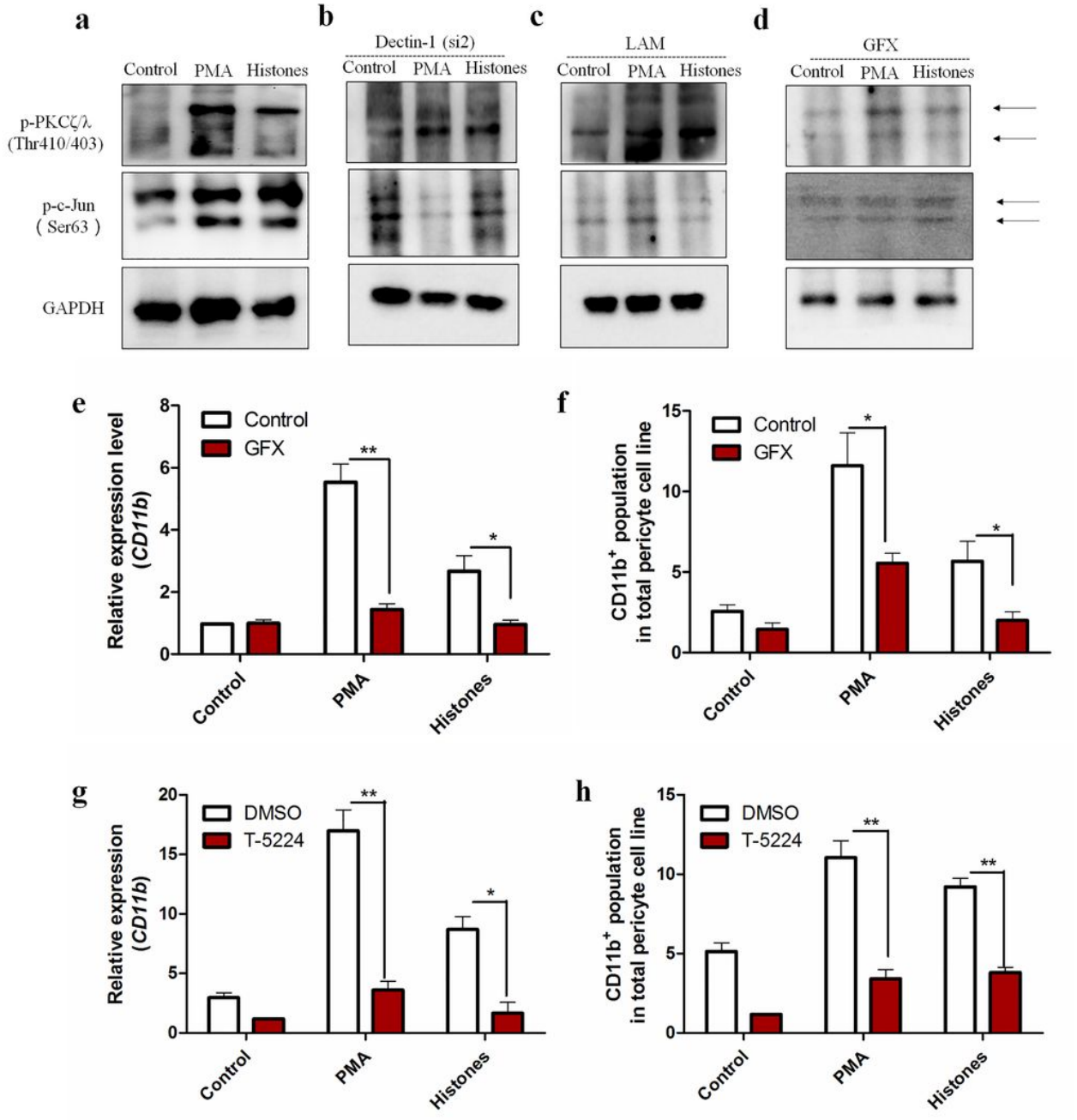

Figure 7

PKC-c-Jun pathways mediated the downstream of by histones/Dectin-1 recognition. a WB analysis of phosphorylated-PKCζ/λ and phosphorylated-c-Jun in MBVP treated with NETs-formed medium (PMA) and Histones (2μg/ml) for 24 hours. b WB analysis of phosphorylated-PKCζ/λ and phosphorylated-c-Jun in Dectin-1 interfered MBVP combined with NETs-formed medium (PMA) and Histones (2μg/ml) treatment for 24 hours. c WB analysis of phosphorylated-PKCζ/λ and phosphorylated-c-Jun in LAM (Dectin-1 antagonist, 100μg/ml) pre-treated MBVP combined with NETs-formed medium (PMA) and Histones (2μg/ml) treatment for 24 hours. GAPDH was utilized as loading control. d WB analysis of

phosphorylated-PKCζ/λ and phosphorylated-c-Jun in GFX (PKC inhibitor, 5μM) pre-treated MBVP combined with NETs-formed medium (PMA) and Histones (2μg/ml) treatment for 24 hours. e Relative expression of CD11b mRNA in MBVP treated with NETs-formed medium (PMA) and Histones (2μg/ml) for 24 hours in the presence of GFX (PKC inhibitor, 5μM). f FACS analysis of CD11+ population in MBVP treated with NETs-formed medium (PMA) and Histones (2μg/ml) for 48 hours in the presence of GFX (PKC inhibitor, 5μM). g Relative expression of CD11b mRNA in MBVP treated with NETs-formed medium (PMA) and Histones (2μg/ml) for 24 hours in the presence of T-5224 (c-Jun inhibitor, 10μM). h FACS analysis of CD11+ population in MBVP treated with NETs-formed medium (PMA) and Histones (2μg/ml) for 48 hours in the presence of T-5224 (c-Jun inhibitor, 10μM). Data are shown as mean±SEM, presented for 3 individual experiments and analyzed by two-tailed unpaired Student's t test. **p<0.01, *p<0.05.

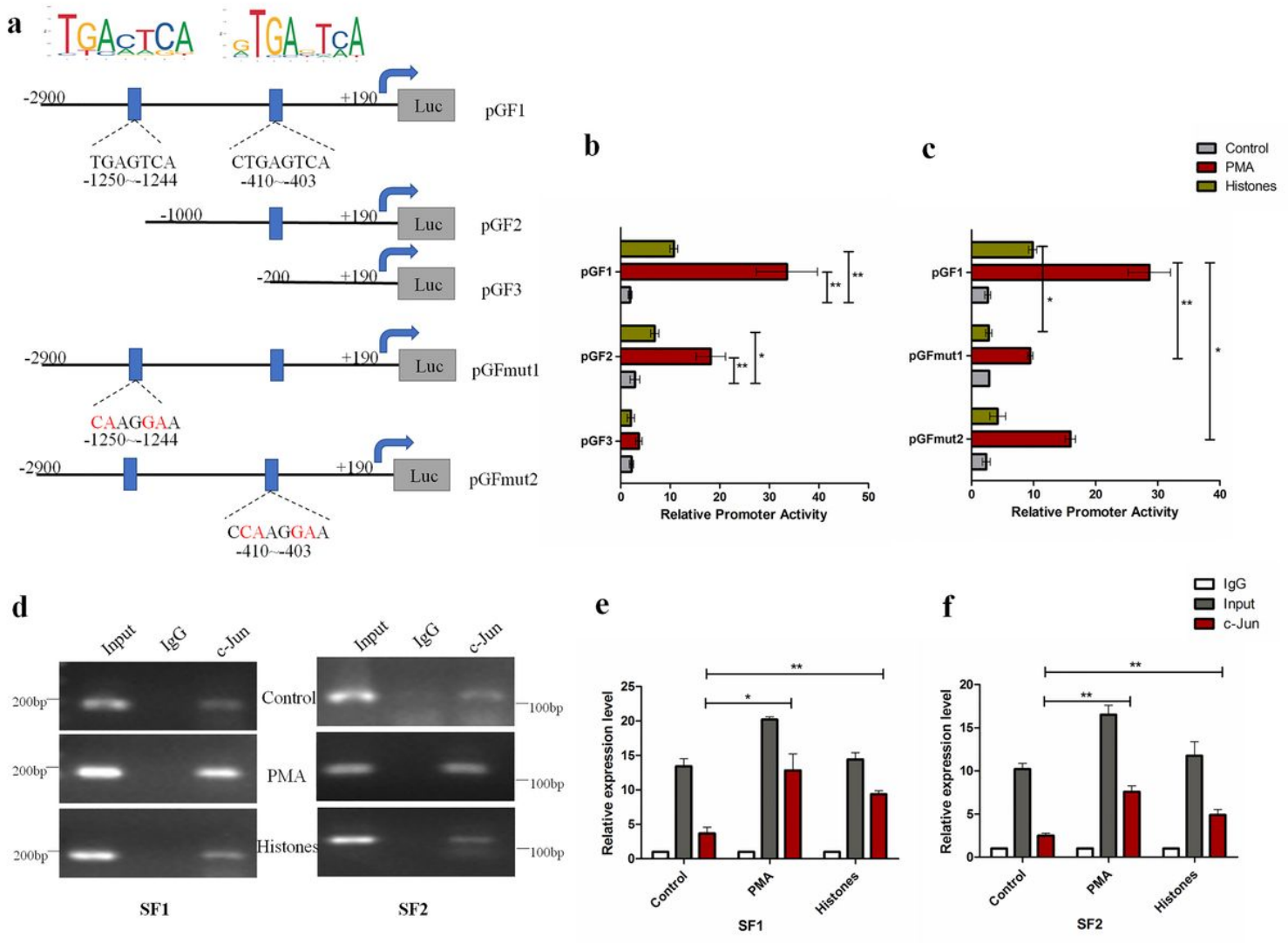

Figure 8

The c-Jun directly enhanced the promoter activity of CD11b gene. a Putative c-Jun binding sequence of mouse CD11b promoter gene. b Luciferace activity of MBVP co-transfected with indicated reporters under specific conditions. c Luciferace activity of MBVP co-transfected with mutated reporters under specific conditions. Control means mixed normal medium with neutrophil-cultured medium (without PMA stimulation), PMA means mixed normal medium with NETs-formed medium induced by PMA (100ng/ml), Histones means normal medium was added with mixed purified histone peptides (H1, H2 and H3, 2μg/ml). All transfected cells were treated under indicated conditions for 24 hours and lysed for dural-luciferace measurement. d CHIP assays of c-Jun binding sequence from CD11b promoter gene. After treating MBVP with indicated conditions for 24 hours, the total chromatin was collected and amplified as input (positive control). Antibody against c-Jun was used for pulling down the biding segments, of which IgG was introduced as negative control. Two pairs of specific primers that covered each binding site were used to amplify SF1 contained segment (-1250~-1244) and SF2 contained segment (-410~-403) respectively within 30 cycles. e&f Realtime-PCR of CHIP products. The quantitative Realtime-PCR was performed with GAPDH as internal reference gene and regarded input from control. Data are shown as mean±SEM, presented for 3 individual experiments and analyzed by two-tailed unpaired Student's t test or ANOVA. **p<0.01, *p<0.05.

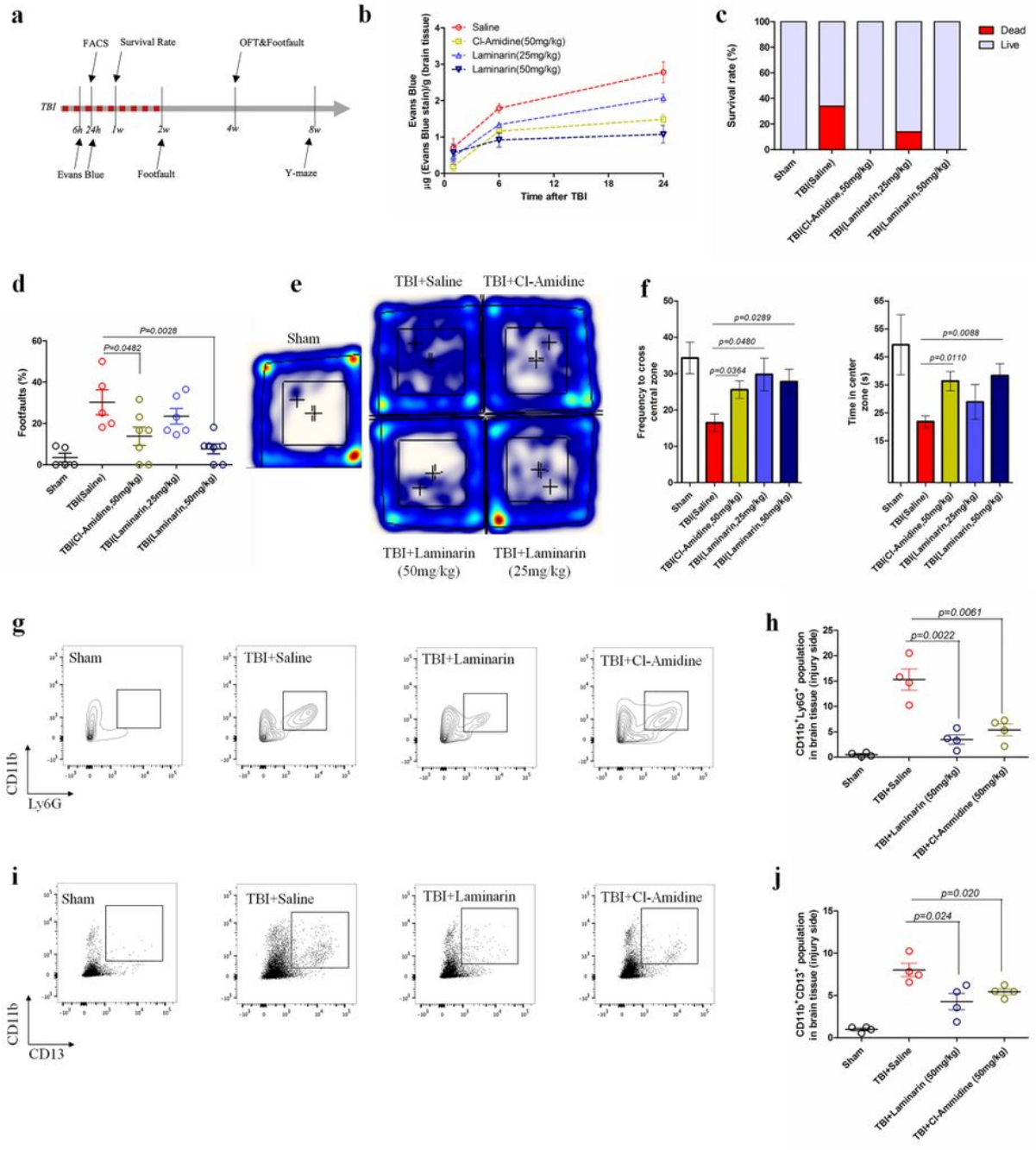

Figure 9

Evaluations of BBB integrity, pericyte activation, neutrophil infiltration and neurological recovery by targeting at NETs-Dectin-1 axis post TBI. a Schematic workflow of animal experiments. After constructing moderate brain impact model, mice were immediately treated with NETs inhibitor Cl-Amidine (50mg/kg) and Dectin-1 antagonist Laminarin (25mg/kg and 50mg/kg) by intraperitoneal injection every three days. Two weeks later, the treatments were terminated and mice were fed without any interferences. b

Quantification of Evan Blue in left brain hemisphere. Evans Blue (2% diluted in saline) was injected into tail vein (4 ml/kg) and allowed to circulate for intended time (30min, 6h and 24 h). The data were presented as (μg of Evans Blue stain)/ (g of injured brain hemisphere). Each group contains 4 mice for each group at intended time point. c Survival rate of each group at the first week after TBI impact in the presence of different treatments. n=6 for Sham, n=10 for TBI. Sham represents the mouse went through the same surgical procedures without impact as control, TBI (saline) represents as placebo group compared with other drug treatment groups. d Footfault evaluation of TBI mice with administration of indicated drugs for 2 weeks. n≥5 for each group. e Heatmap of mice movement in OFT assessment at 4 weeks after moderate TBI impact in the presence of different treatments. f Quantification of OFT assessment (e) in the aspects of frequency to cross central zone and time that mice spent in center zone. n≥5 for each group. g FACS analysis of infiltrated neutrophils (CD45+CD11b+LY6G+) from injured brain tissue at 24 hours in TBI mice treated with indicated drugs (Laminarin, 50mg/kg; Cl-Amidine, 50mg/kg). n=4 for each group. h Quantification of (g). i FACS analysis of activated brain pericyte (CD45-CD11b+CD13+) from injured brain tissue at 24 hours in TBI mice treated with indicated drugs (Laminarin, 50mg/kg; Cl-Amidine, 50mg/kg). n=4 for each group. j Quantification of (i). Data are presented as mean±SEM, and analyzed by One-way ANOVA. The animal numbers and p values of each group are shown in figures and intended legends.

Supplementary Files

This is a list of supplementary files associated with this preprint. Click to download.

- Tables.docx
- FigureS1.tif
- FigureS2.tif
- FigureS3.tif
- FigureS4.tif
- FigureS5.tif
- FigureS6.tif
- FigureS7.tif
- FigureS8.tif